SAND2019-3428PE

Impact of Multiscale Heterogeneity on Mechanical Behavior of Mancos Shale

Hongkyu Yoon

Geomechanics Department

Sandia National Laboratories

Sandia National Laboratories

Exceptional service in the national interest

National Nuclear Security Administration

Sandia National Laboratories is a multimission laboratory managed and operated by National Technology and Engineering Solutions of Sandia, LLC, a wholly owned subsidiary of Honeywell International, Inc., for the U.S. Department of Energy's National Nuclear Security Administration under contract DE-NA-0003525.

Acknowledgments

- Laboratory Directed Research and Development program at Sandia National Laboratories
- U.S. Department of Energy Office of Basic Energy Sciences, Division of Chemical Sciences, Geosciences, and Biosciences
- Thomas Dewers, Mathew Ingraham, Bill Mook (SNL)
- Peter Mozley, Oh-Tark Kwon (NMT)

SANDIA NATIONAL LABORATORIES OVERVIEW

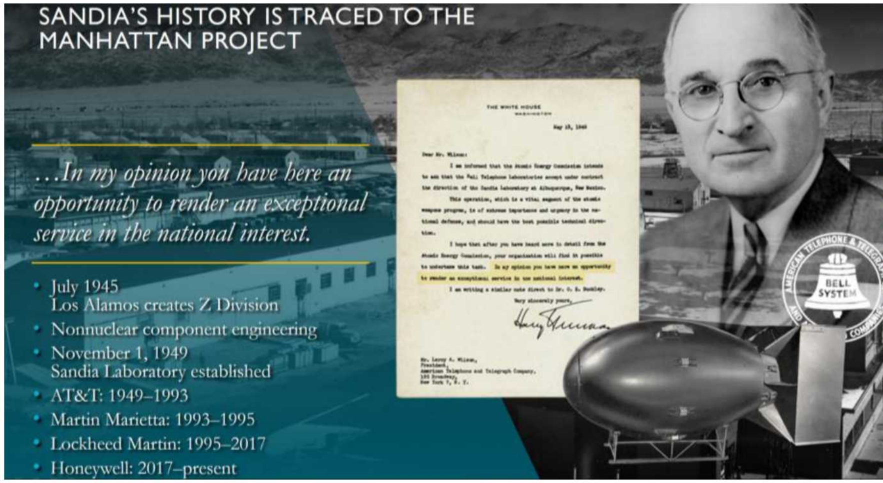

SANDIA ADDRESSES NATIONAL SECURITY CHALLENGES

SANDIA'S BUDGET and WORKFORCE

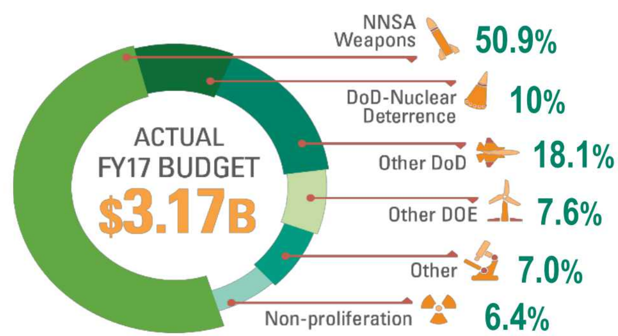

12,256 EMPLOYEES	10,940 New Mexico	1,316 California

Subsurface Energy Activities

- Subsurface energy technologies typically involve the change of fluid flow, stress, thermal, chemical (aka THMC) status in fractured and porous media
  - **Unconventional resources recovery**
  - Disposal of wastewater and nuclear waste
  - Subsurface carbon and compressed gas storage
- To improve subsurface energy activities and reduce adverse risks (e.g., induced seismicity and environmental impact), current understanding of (thermo-, chemo-)poro-mechanics needs to be improved
- Mesoscale analysis – linking discrete and complex pore-scale behavior to continuum (macroscale) reservoir response – is key, yet remains elusive as a result of the extreme heterogeneity and resulting scale dependence.

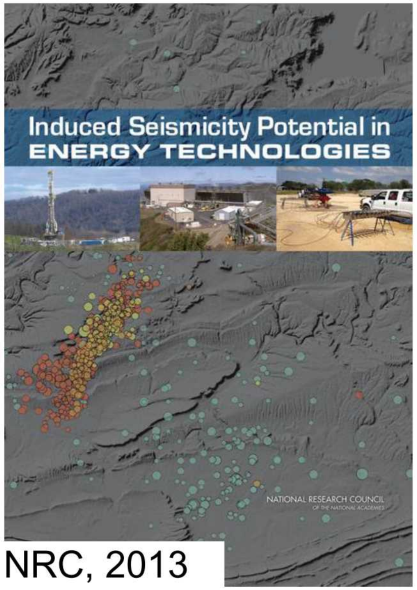

NRC, 2013

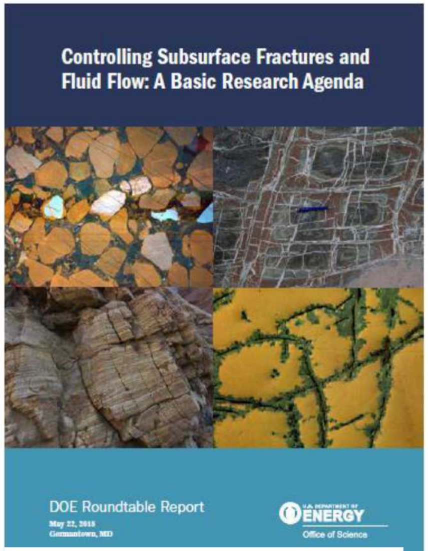

DOE BES Report, 2015

Multiscale Heterogeneity in Compositions, Pore structure, and Mechanical Properties

► Understand how heterogeneity, pores, cracks, flaws etc. contribute to shale poromechanics over scales and provide physical basis for core-scale measured deformational and transport constitutive behavior

► Develop novel techniques and workflow for a linked imaging, experimental, and modeling-based advancement of shale poromechanics

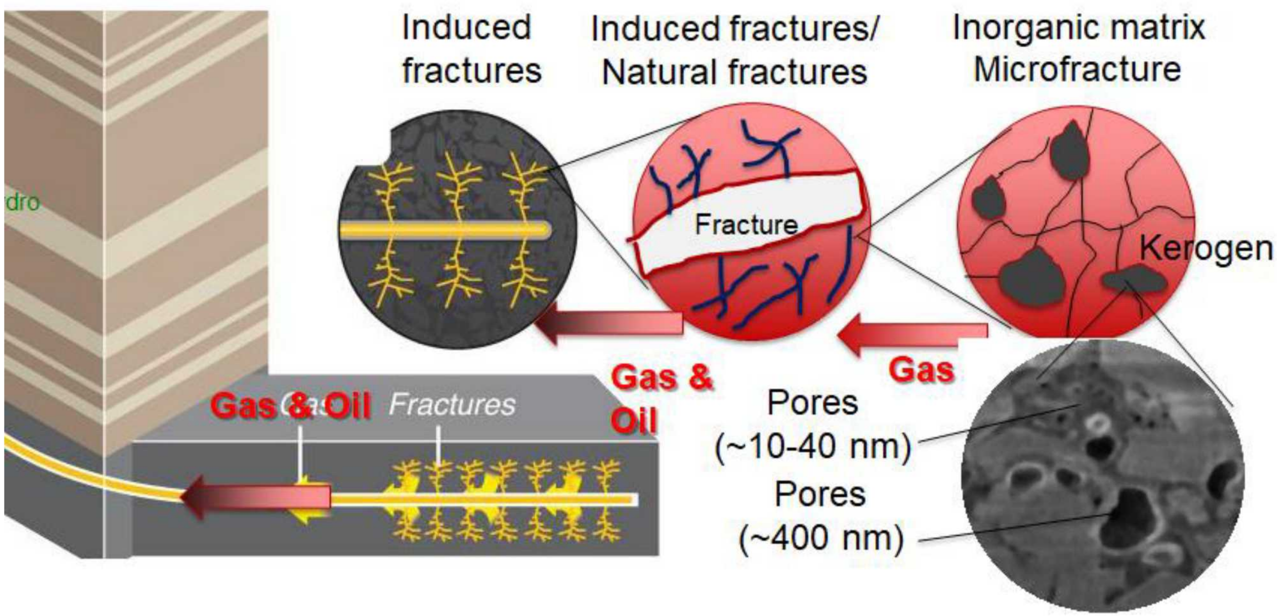

Clay-rich area,
64 nanoindentations
Load-displacement

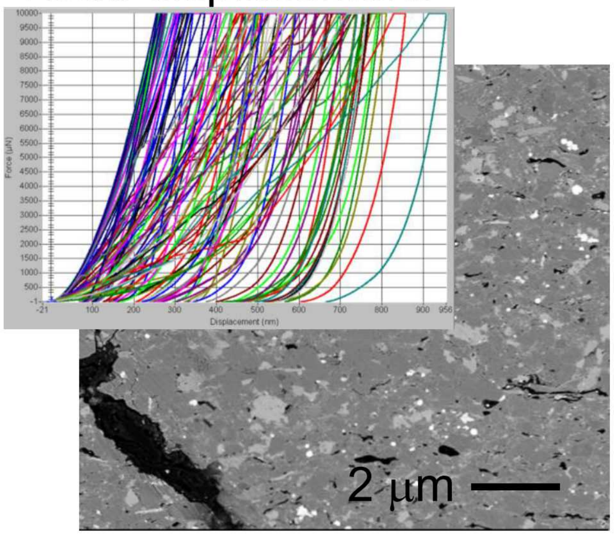

Integrated Approach

- **40 cm diameter core of Mancos Shale**
  - Interlaminated fine mud, medium/ coarse mud, and very fine sand
  - 1-3 mm laminae
  - Parallel lamina, wavy lenticular lamina, ripple forms, and bioturbation
- **Mineralogical and textural characterization**
  - Macroscopic
  - Optical petrography/microscopy
  - Micro-CT
  - XRD/X-ray Microprobe
  - Small Angle Neutron Scattering
  - Focused Ion Beam-SEM
  - Back-Scattered Electron Microscopy
  - MAPS Mineralogy
- **Mechanical Experiments**
  - Uni-/Tri-axial compression (1x2")
  - Brazilian Test (1x0.5")
  - Nanoindentation
- **Computational modeling**

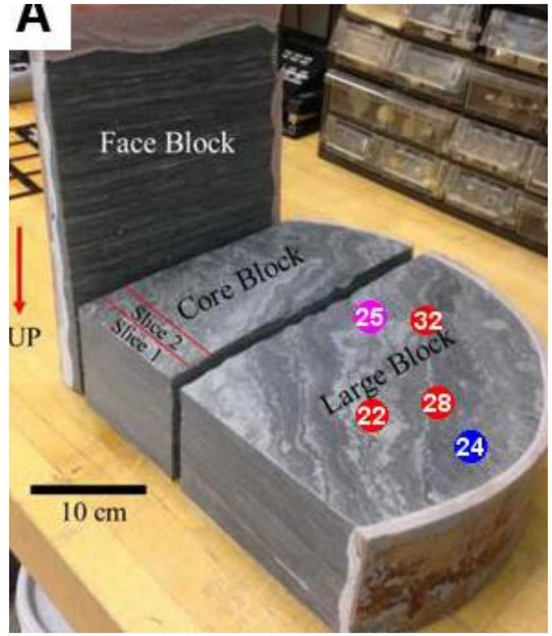

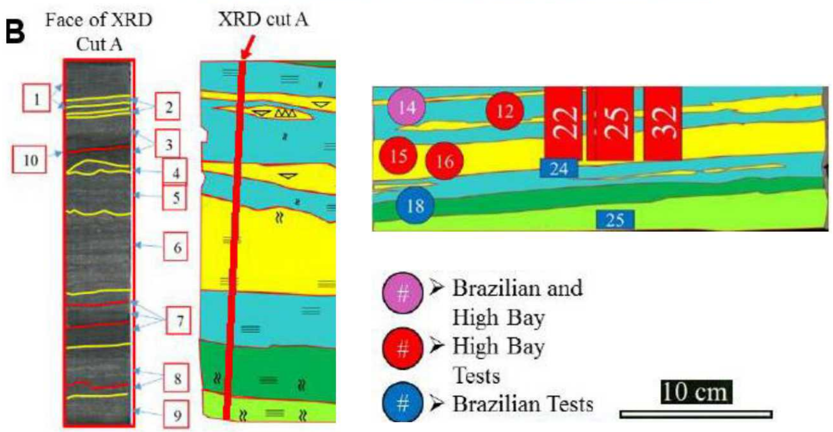

Yoon et al. (AAPG, Memoir 2019, in press)
Dewers et al. (AGU, Monograph, 2019)

Integrated Approach

- **Mineralogical and textural characterization**
  - Macroscopic
  - **Optical petrography/microscopy**
  - Micro-CT
  - **XRD/X-ray Microprobe**
  - Small Angle Neutron Scattering
  - Focused Ion Beam-SEM
  - **Back-Scattered Electron Microscopy**
  - **MAPS Mineralogy**
- **Mechanical Experiments**
  - Uni-/Tri-axial compression (1x2")
  - Brazilian Test (1x0.5")
  - Nanoindentation
- **Computational modeling**

Multiscale characterization of physical, chemical, and mechanical heterogeneity of nano-porous geomaterials

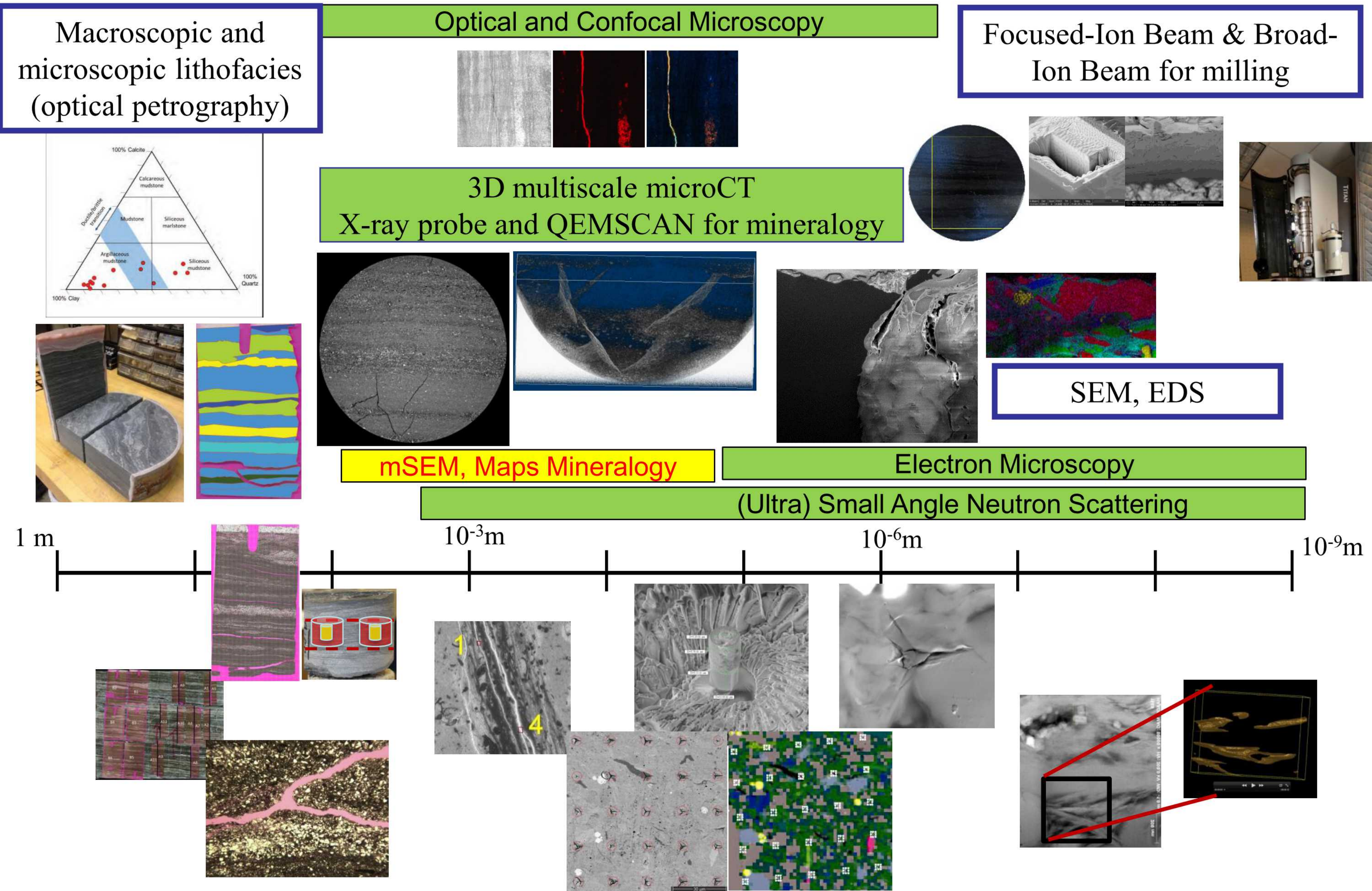

MAPS Mineralogy

- **SEM-based automated mineralogical measurement, analysis, data integration**
  - – Collection, overlay and re-registration of multiple images from different modalities
  - – SEM, SEM-EDS, optical, CL, EBSD
  - – QEMSCAN measurement algorithms
- **Mineral identification**
  - – Spectral matching
  - – Each pixel – single/multiple minerals
  - – Elemental substitutions
  - – Simultaneous mineral element and count maps

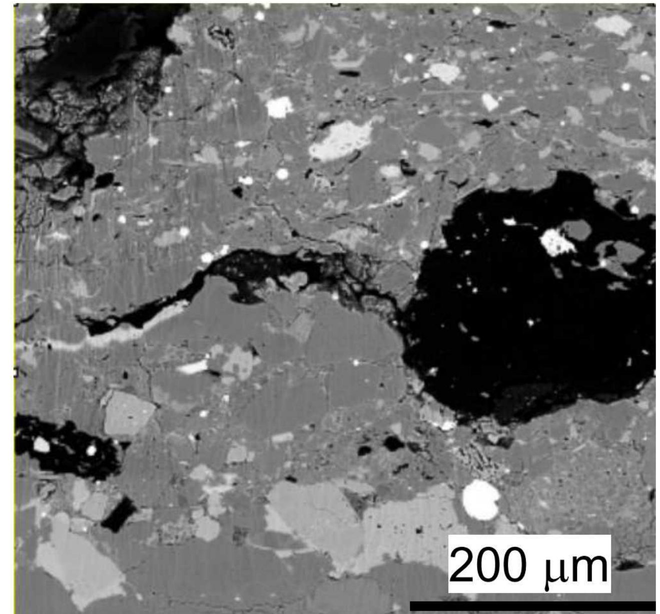

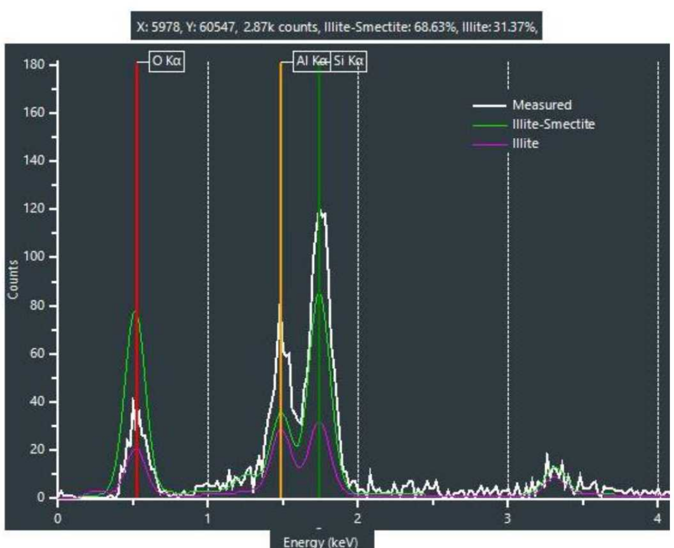

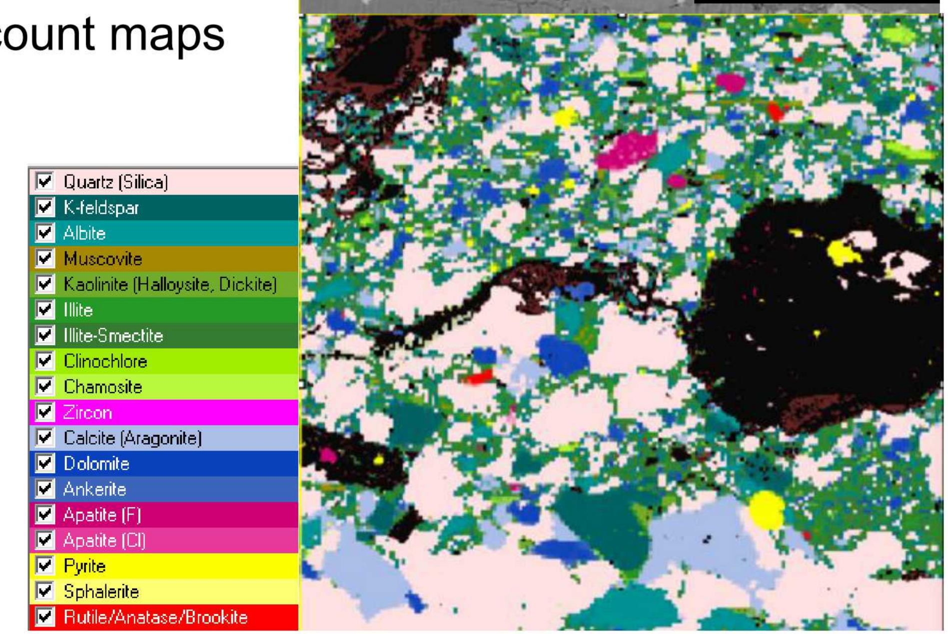

Mineralogy Mapping

Ion-milling polished Mancos
(1 inch diameter)

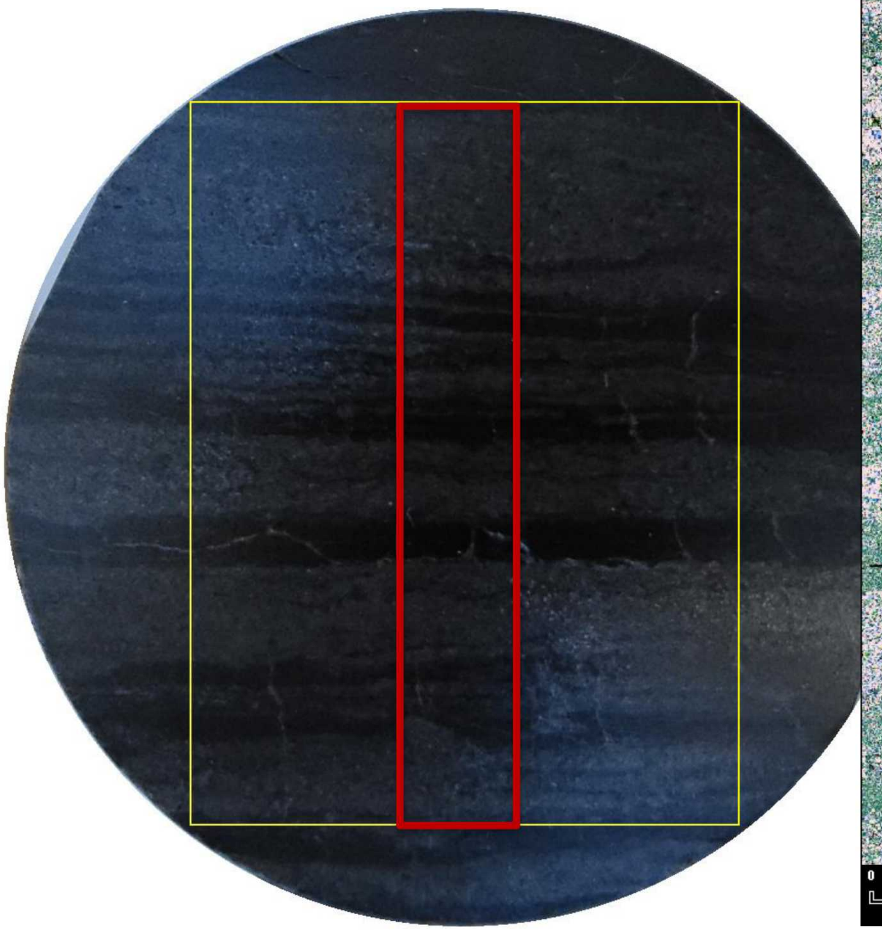

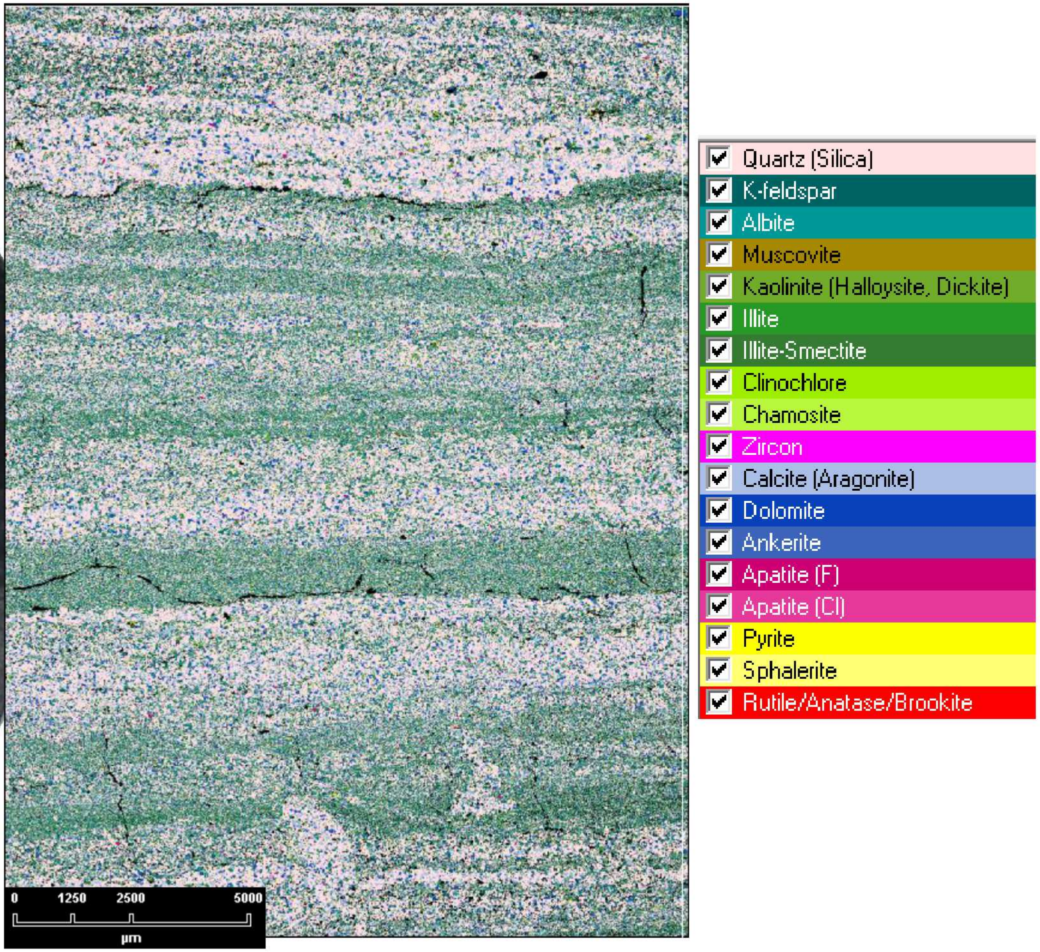

Yellow Box (1.45 x 1.98 cm): BSE @ 1μm & MAPS @ 10μm
Red box (0.18 x 1.98 cm): BSE @ 0.2μm & MAPS @ 2μm

Mineralogy Mapping: Scale/methods dependent

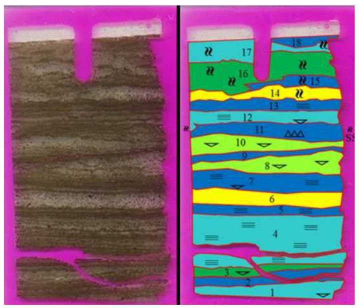

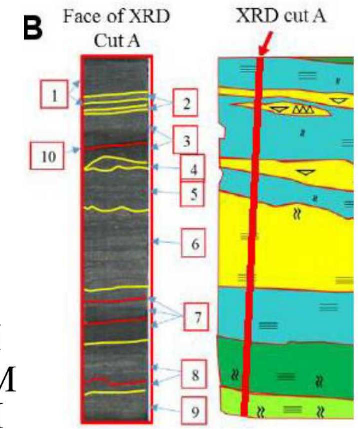

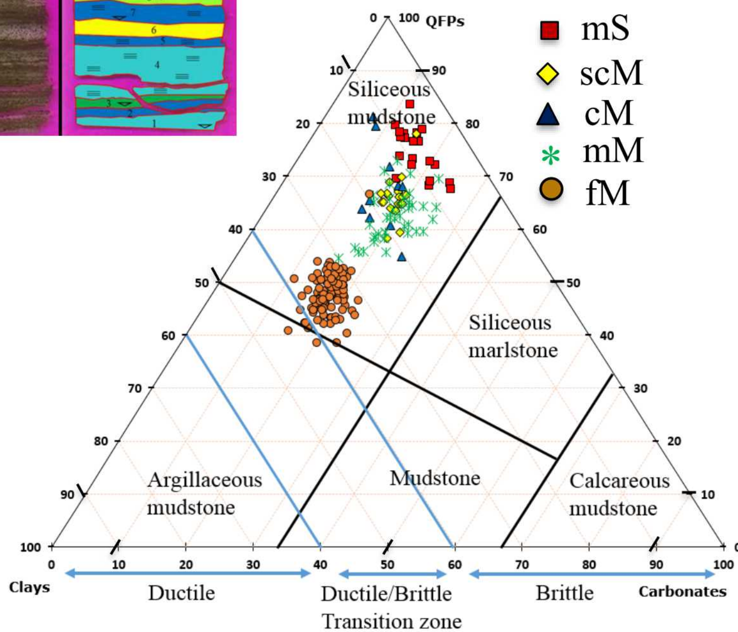

MAPS
(2 and 10 microns)

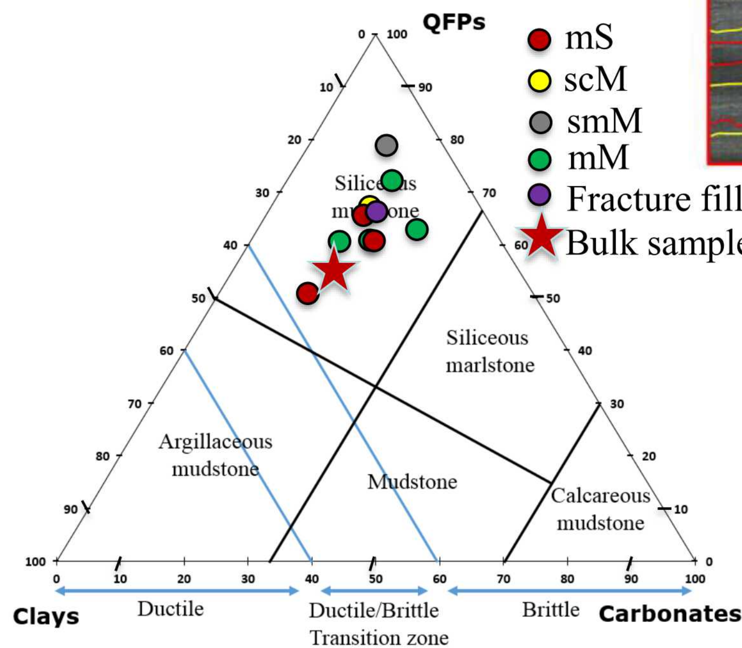

XRD
(10+1 samples)

Yoon et al. (AAPG, Memoir 2019, in press)

Mineralogy Mapping: Scale/methods dependent

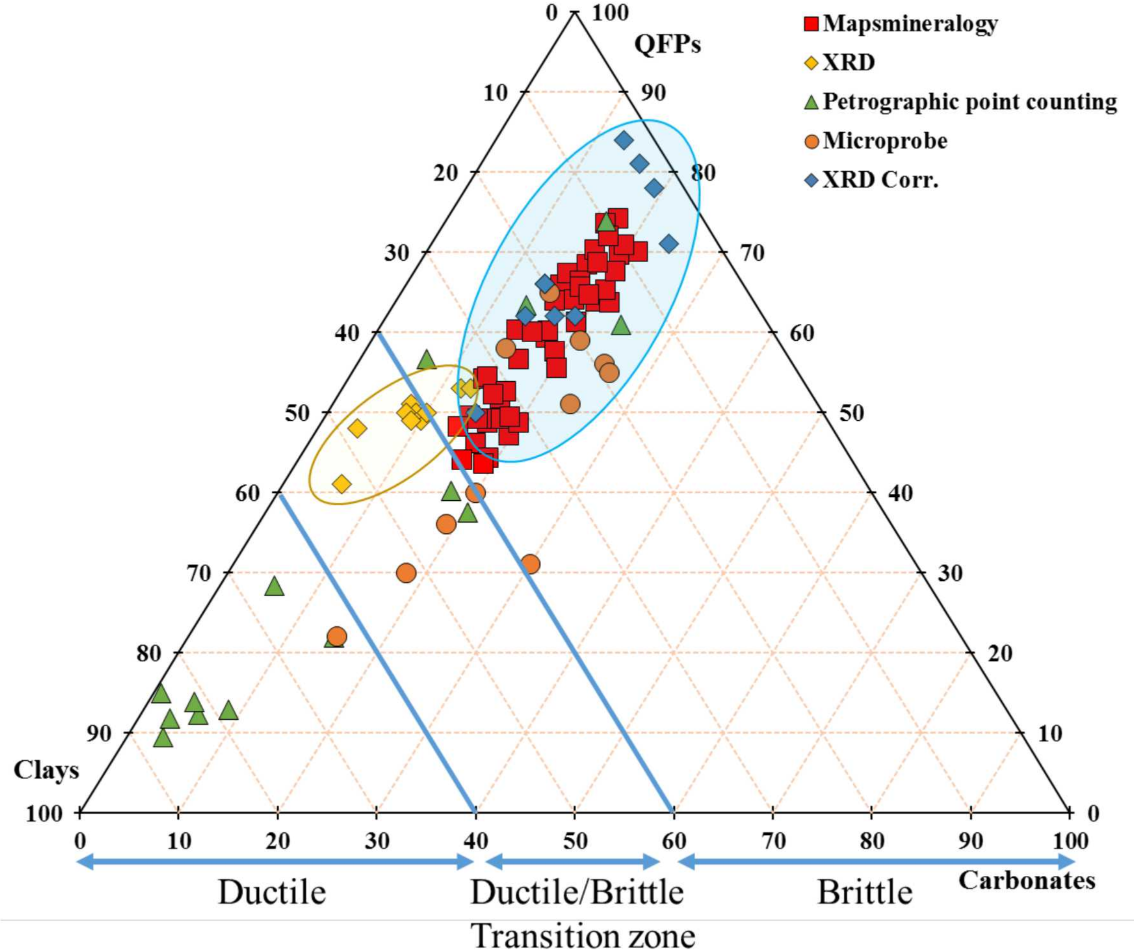

Kwon (@NMT, MS work, 2018)

Influence of geological attributes on mechanical properties

Micro-lithofacies

mS

scM

cM

mM

fM

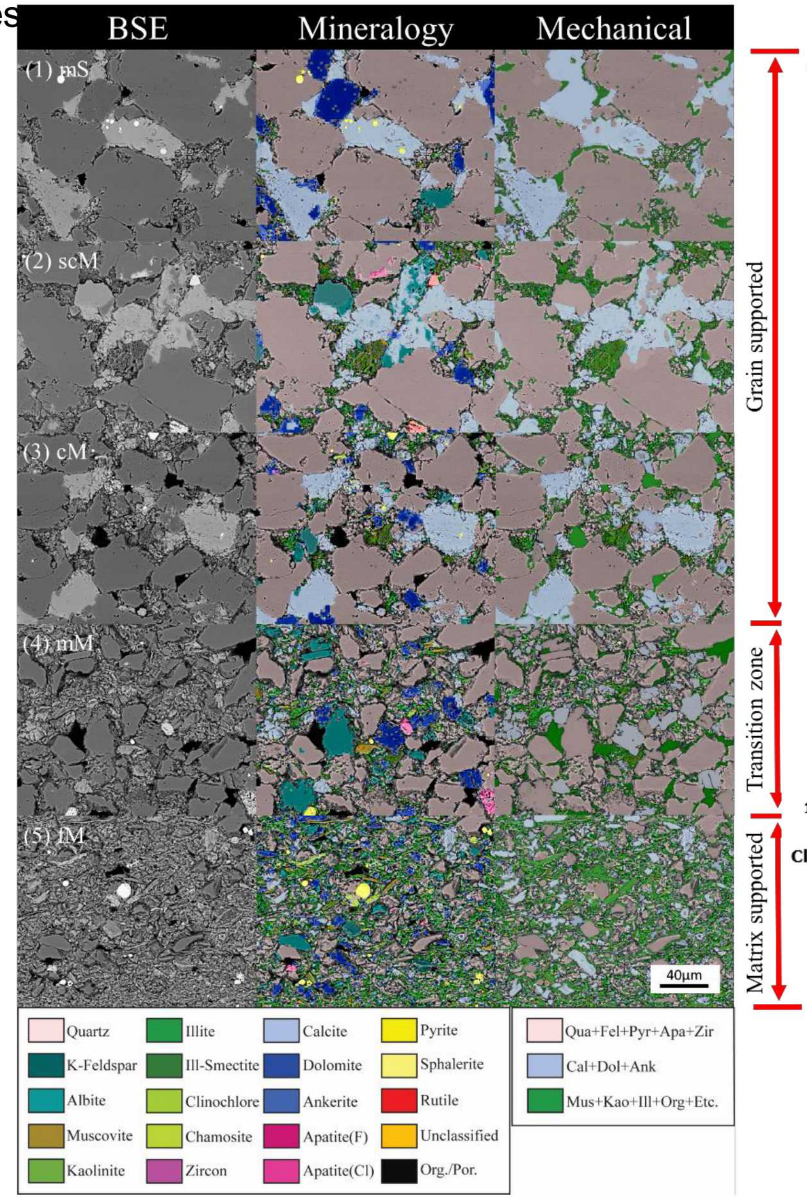

Mineral Assemblages

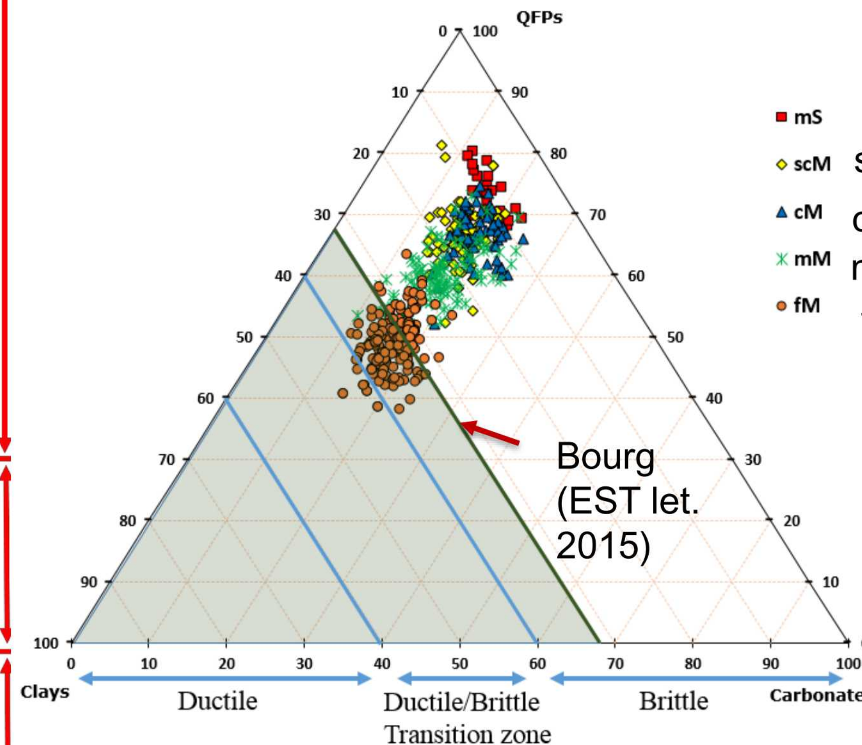

mS
scM
cM
mM
fM

Ulmer-Scholle et al. (2014)

Kwon (@NMT, MS work, 2018)

Integrated Approach

- **Mineralogical and textural characterization**
  - Macroscopic
  - Optical petrography/microscopy
  - Micro-CT
  - XRD/X-ray Microprobe
  - Small Angle Neutron Scattering
  - Focused Ion Beam-SEM
  - Back-Scattered Electron Microscopy
  - MAPS Mineralogy
- **Mechanical Experiments**
  - **Tri-axial compression (1x2”)**
  - **Brazilian Test (1x0.5”)**
  - Nanoindentation
- **Computational modeling**

Conceptual Model of Anisotropic Layered System

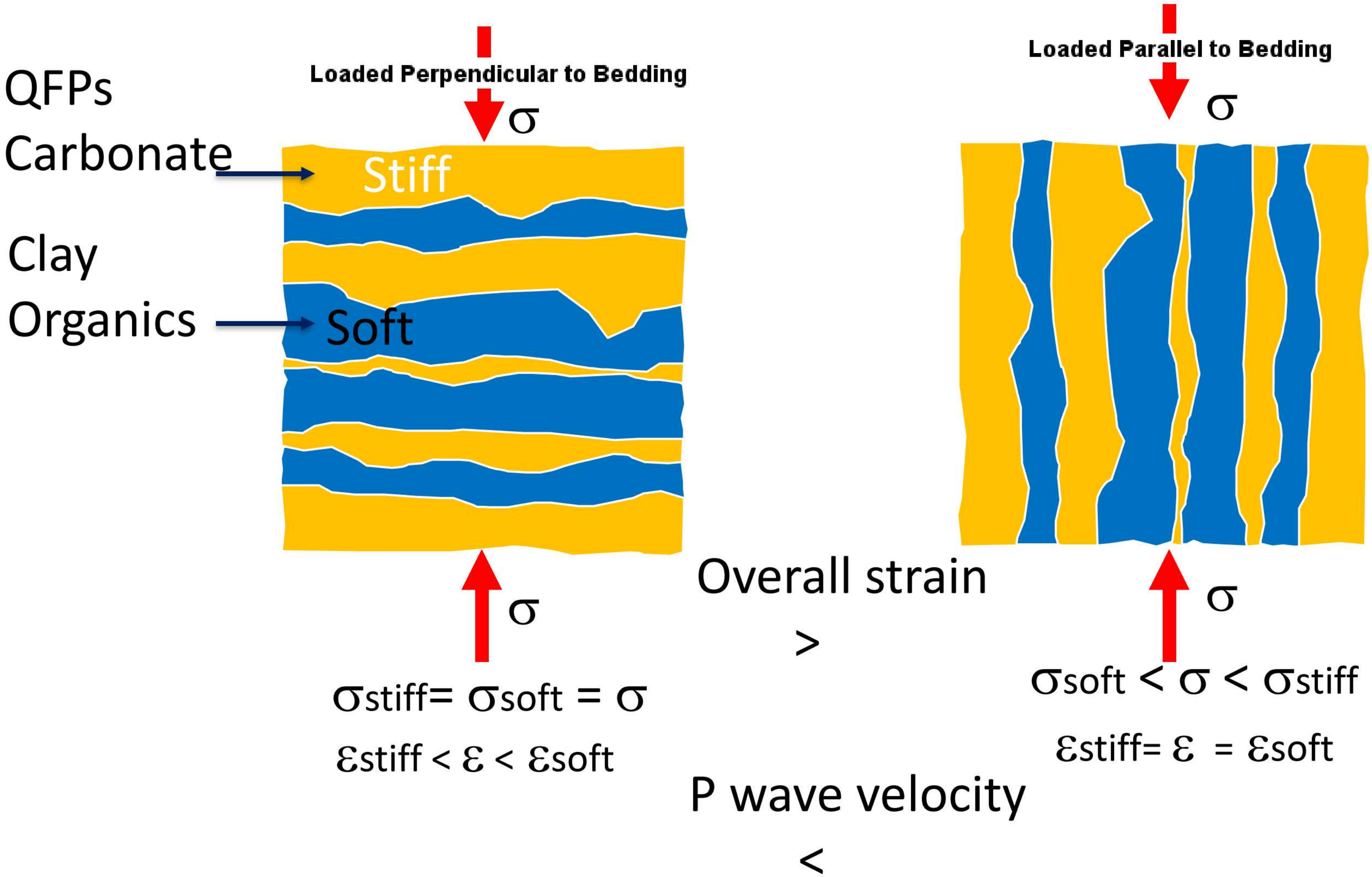

Axisymmetric Compression Testing

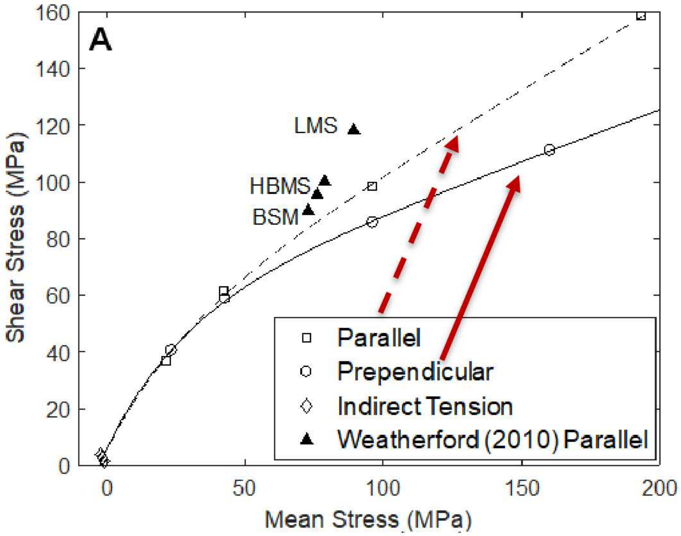

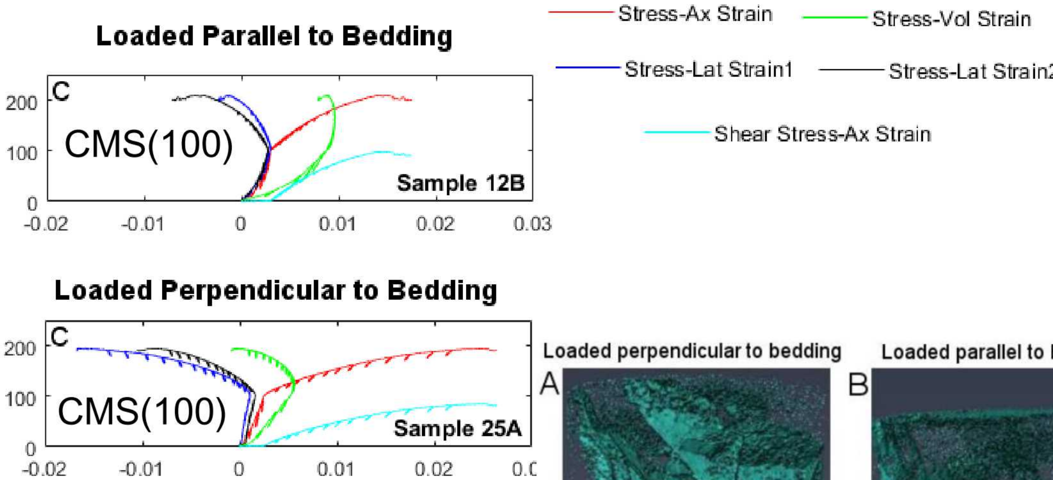

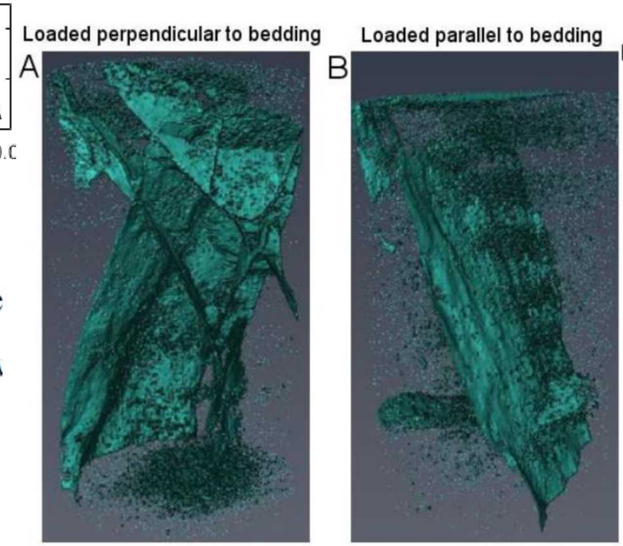

Segmented MicroCT images

	Confined (MPa)		Axial Stress	Mean Stress	Shear Stress	Fracture Angle (\
15B	CMS (50)	Parallel	113.00	42.20	61.31	13.5
28A	CMS (50)	Perpendicular	110.64	42.80	58.75	15.5
12B	CMS (100)	Parallel	209.59	96.09	98.30	23.5
25A	CMS (100)	Perpendicular	195.07	96.20	85.62	30
14B	CMS (200)	Parallel	376.37	193.42	158.44	27.5
22A	CMS (160)	Perpendicular	288.64	160.31	111.14	35.5

CMS: Constant Mean Stress

Yoon et al. (AAPG, Memoir 2019, in press)

Axisymmetric Compression Testing

Horizontal slice through the central part of sample

A. Loaded parallel to bedding (15B)

One primary & two secondary fractures

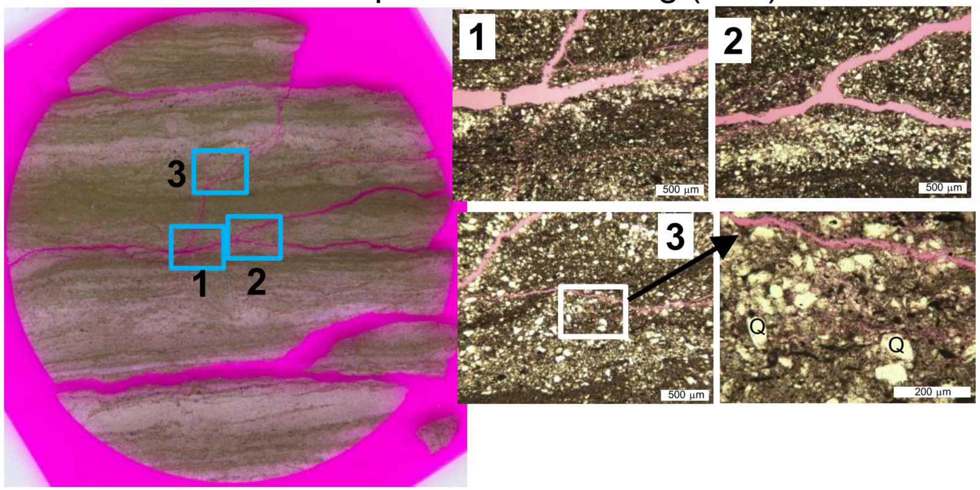

Fracture intersection & bifurcation with small aperture microfractures

Microfracture propagation in between quartz grains

B. Loaded perpendicular to bedding (28A)

Curved main fracture

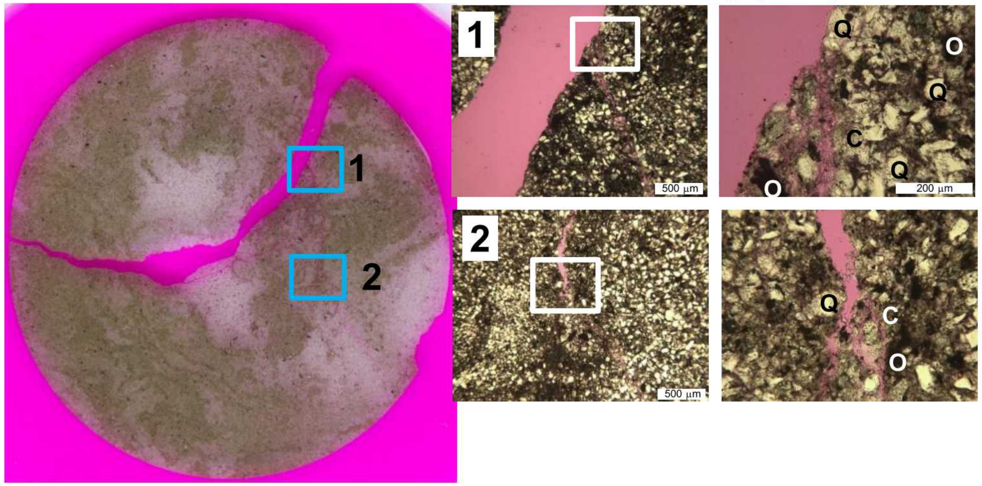

Microfracture patterns in between quartz grains

Indirect Tension Results

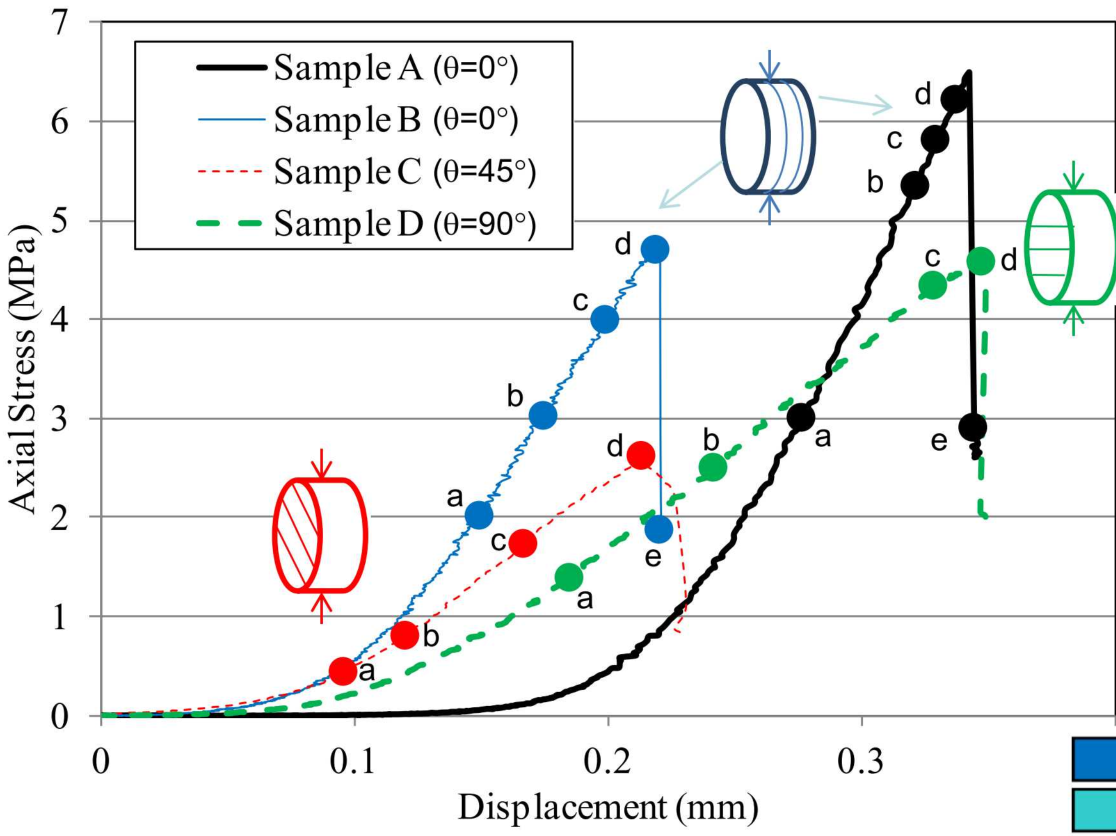

$$\sigma_t = \frac{2P}{\pi D t}$$

P: Loading

D: Diameter

t: thickness

Na et al. (JGR 2017)

Numerical Simulations of Brittle Fracturing

- Phase field model for crack representation (Heister et al,2015)
- Shale is modeled as two-constituent brittle materials with stiff and soft layers:
  - Young's Modulus
  - (Pore pressure)
  - (Chemo-mechanical coupling)

Crack phase field (φ)

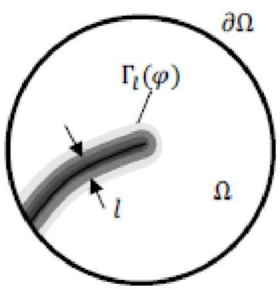

Differential Equations Analysis Library.II (Bangerth et al., 2007; 2013)

DEAL.II Open Source Finite Element Library

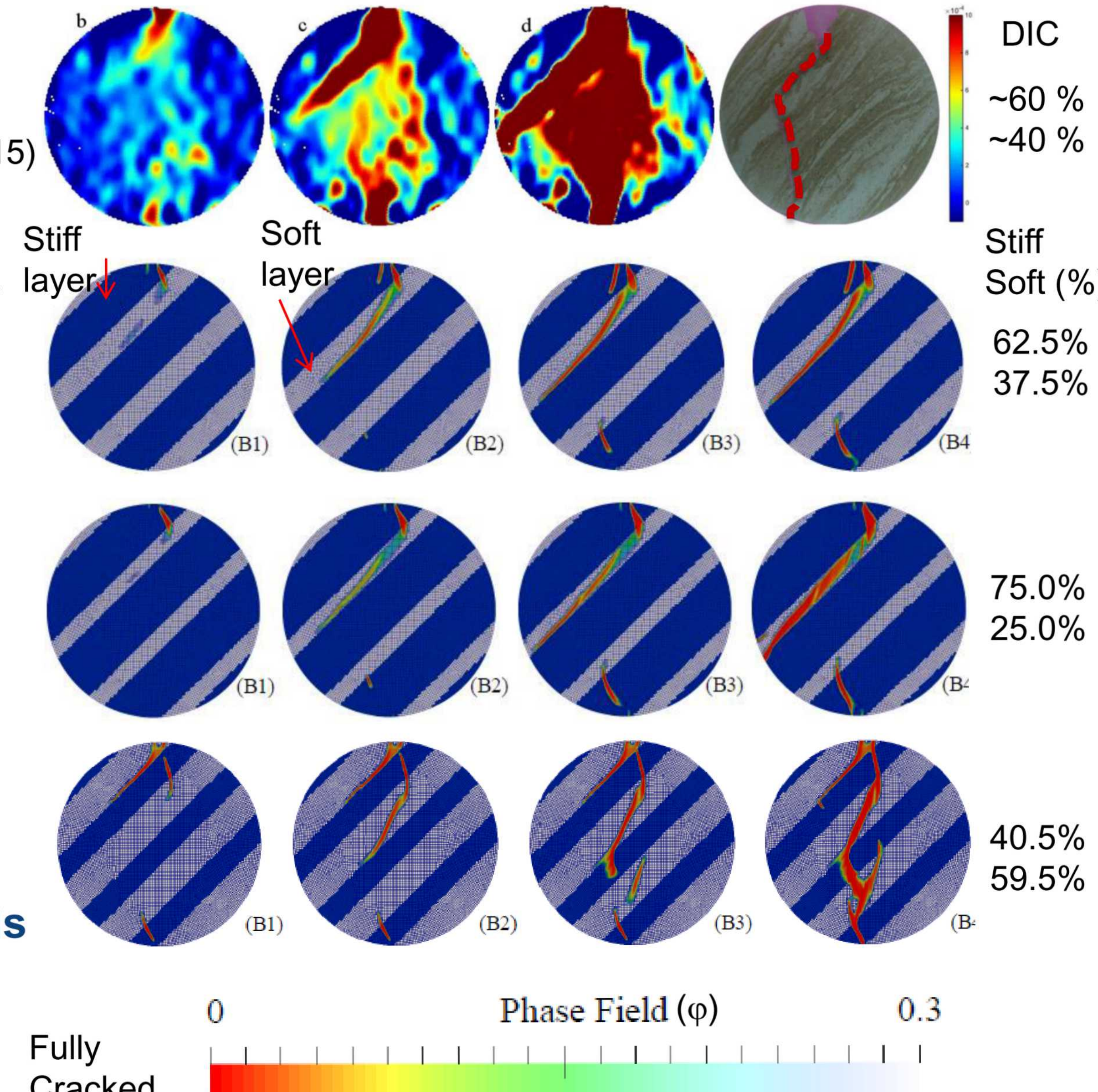

Na et al. (JGR 2017)

Effective Properties of Heterogeneous Materials

- Transversely isotropic effective medium for elastic parameters (Berryman, 1998)
  - Spatial homogenization procedure leads to much simpler crack patterns than those from the layered isotropic materials
  - Crack paths in the effective medium are less tortuous due to (probably) filtering out mesoscopic information via homogenization
  - Smaller surface area created by the fracture process yields the reduced tortuous crack paths with a diminished amount of energy dissipation (much higher effective fracture toughness)

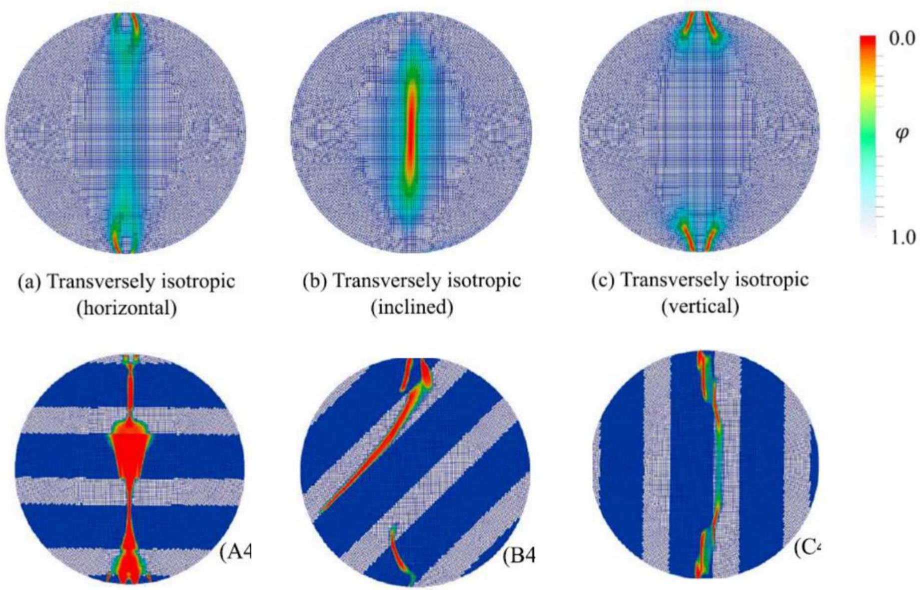

(a) Transversely isotropic (horizontal) (b) Transversely isotropic (inclined) (c) Transversely isotropic (vertical)

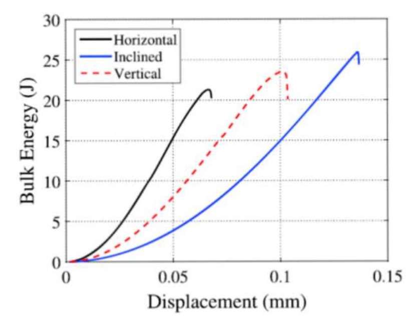

Transversely Isotropic

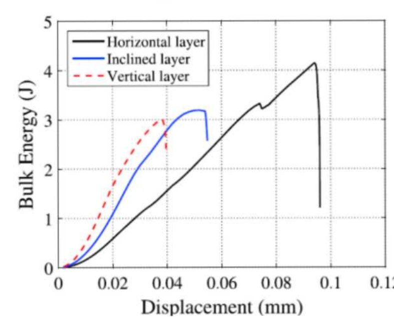

Layered Isotropic

Na et al. (JGR 2017)

Integrated Approach

- **Mineralogical and textural characterization**
  - Macroscopic
  - Optical petrography/microscopy
  - Micro-CT
  - XRD/X-ray Microprobe
  - Small Angle Neutron Scattering
  - Focused Ion Beam-SEM
  - Back-Scattered Electron Microscopy
  - MAPS Mineralogy
- **Mechanical Experiments**
  - Tri-axial compression (1x2”)
  - Brazilian Test (1x0.5”)
  - **Nanoindentation**
- **Computational modeling**

NanoIndentation

- **Depth sensing/instrumented indentation**
  - – highly accurate load-displacement record
  - – Analytical models to determine modulus, hardness and other mechanical properties using the load-displacement data

Berkovich indenter

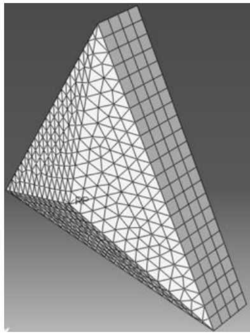

- **Analytical concept**
  - – Purely elastic deformation upon initial unloading
  - – Contact between a rigid indenter and homogeneous isotropic elastic half spacing
  - – Compliance of the sample and indenter tip – springs in series
  - – Hardness = load/contact area
  - – Elastic modulus determined by stiffness (S)

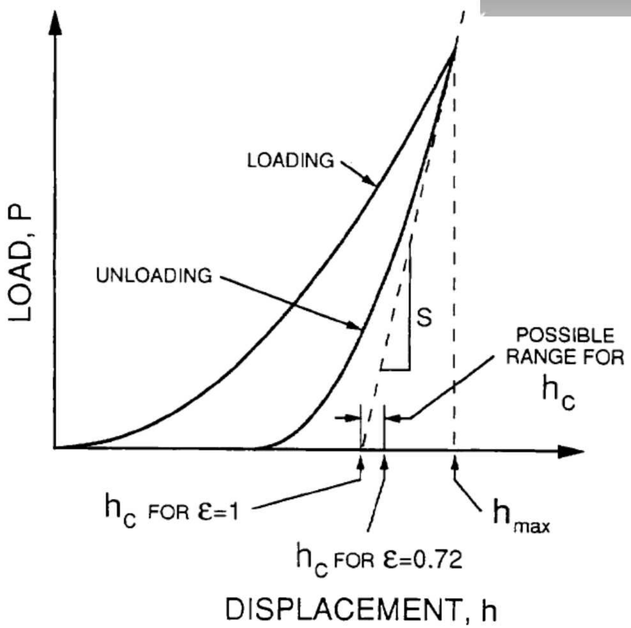

Oliver & Pharr (1992)

- **Dynamic Modulus Analysis at nm scale**

Initial Indentation Results

Indentation array: 16 x 16, 20 um spacing
[Hysitron TriboIndenter 900]
Indentation strain rate = 0.1 (Oliver et al., 1997)
(current change in displacement/current total disp.)
Maximum load = 10 mN

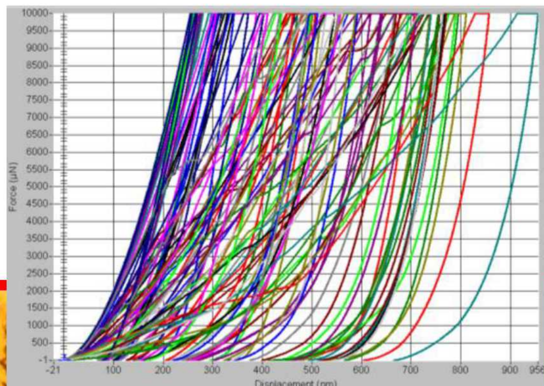

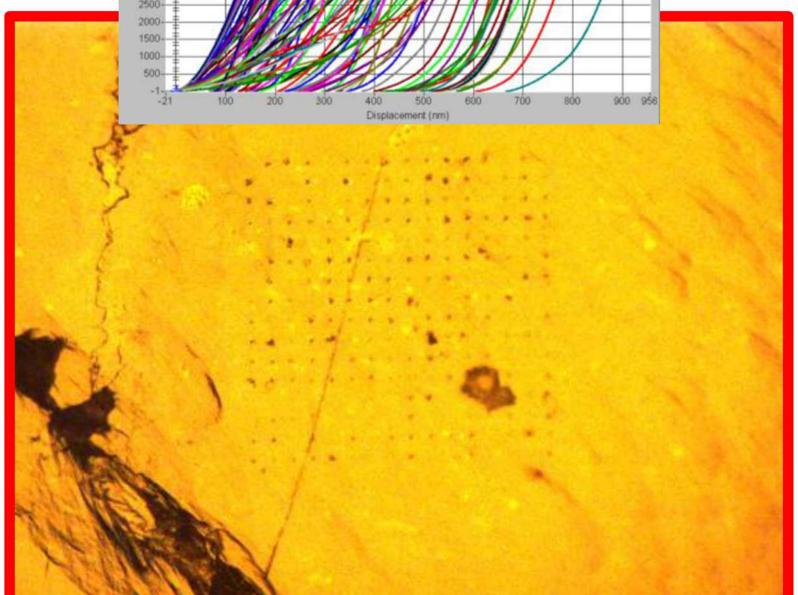

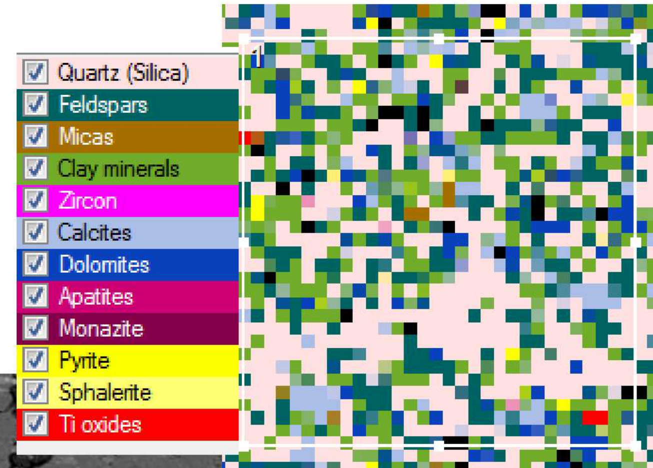

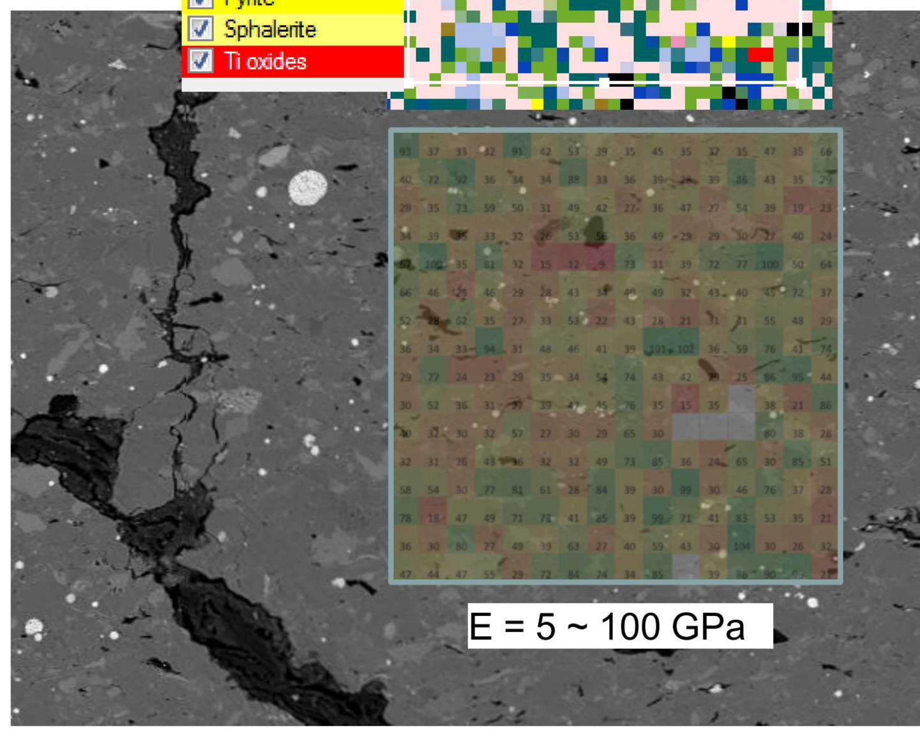

Multiscale Indentation Testing

Loading-unloading cycle

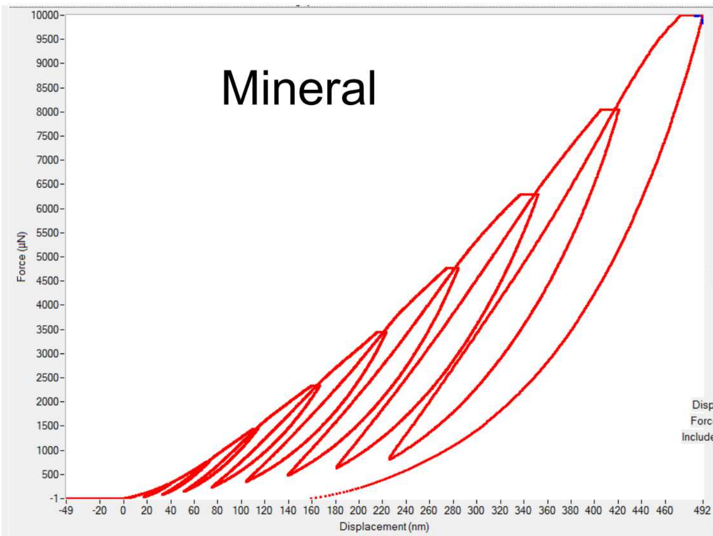

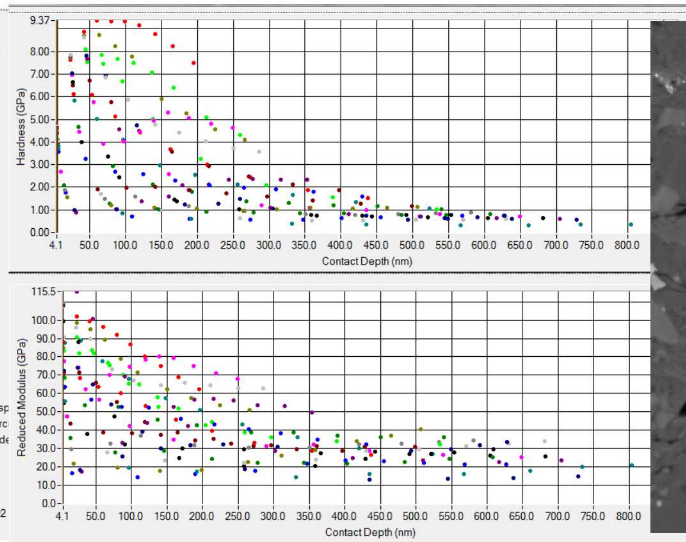

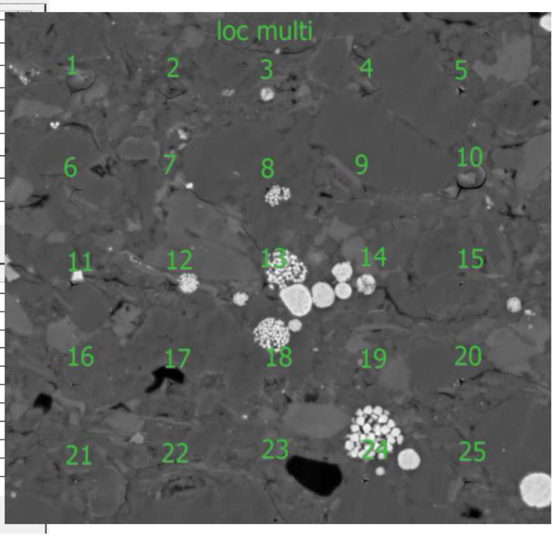

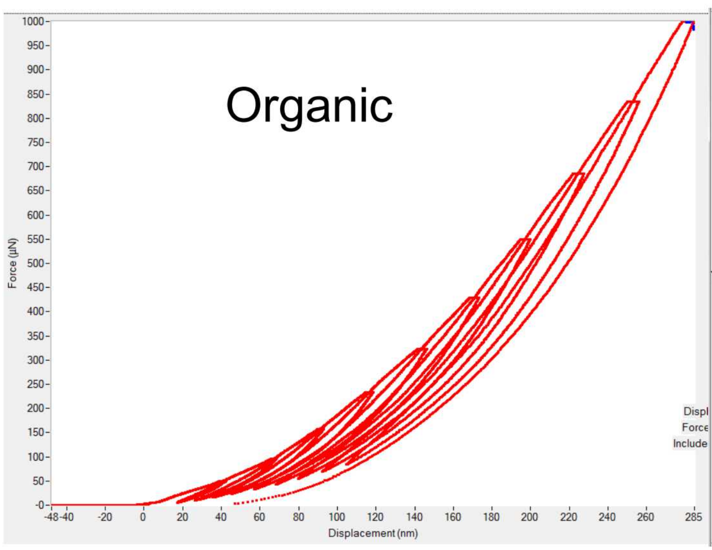

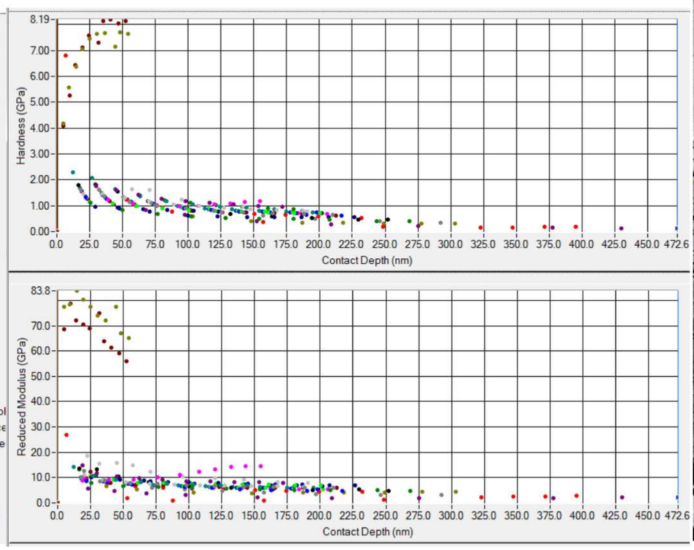

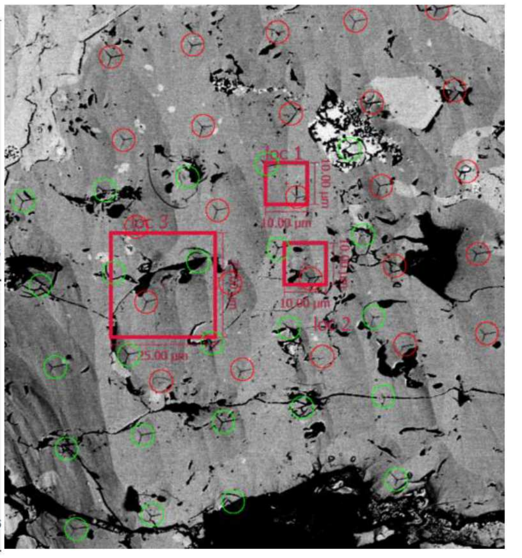

Multiscale Indentation Testing

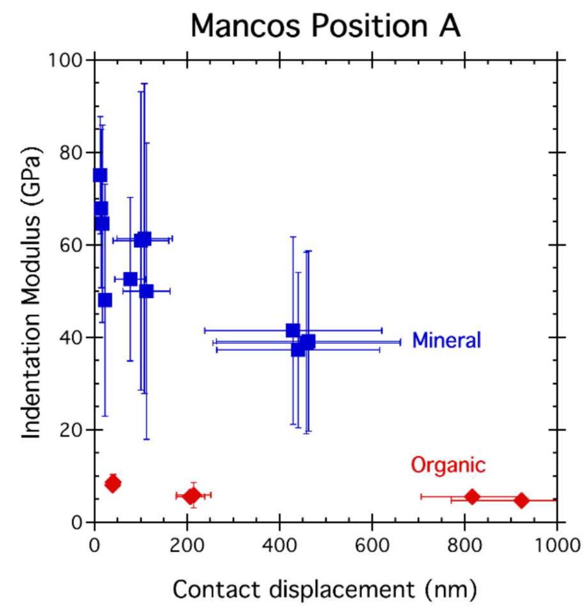

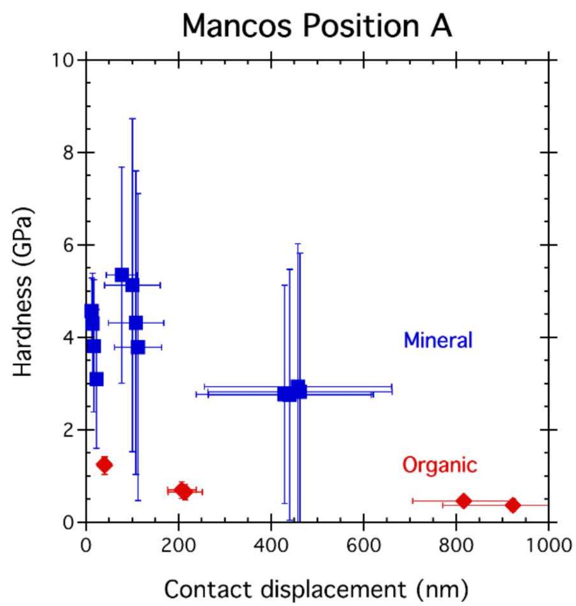

Distributed arrays

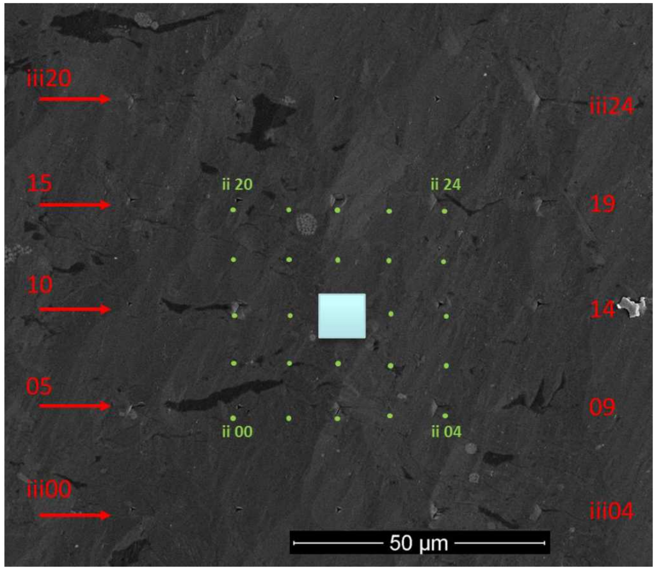

Indentation key	Array dimension	indent spacing	Max Load
i	8x8 um	2 um	0.1 mN
ii	40x40 um	10 um	1 mN
iii	80x80 um	20 um	10 mN

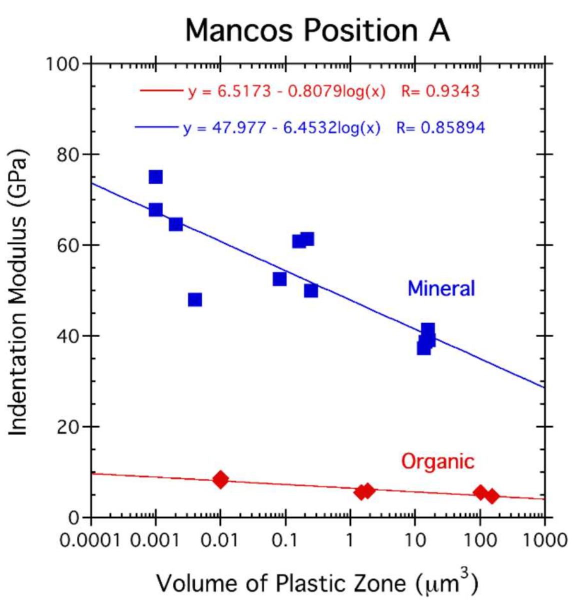

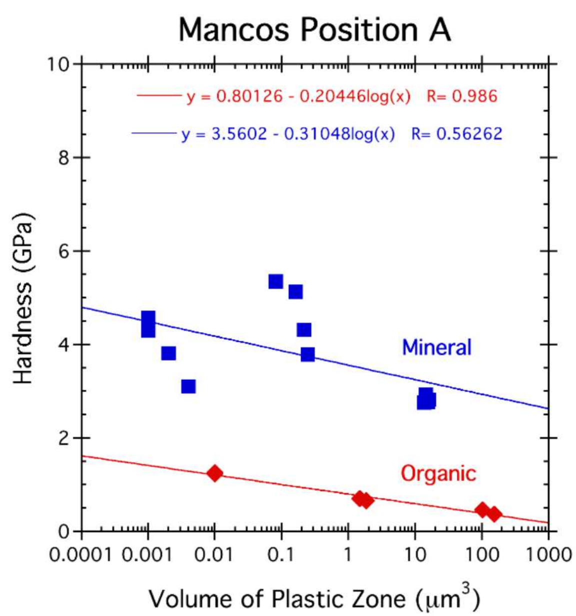

Estimate plastic zone radius

$$\frac{R_p}{\delta_m} = -12.907\frac{H}{E_r} + 4.5451 \qquad \frac{H}{E_r} < 0.35$$

Chen & Bull, Surface & Coatings Technology (2006) 4289–4293.

Effect of Mineralogy on Mechanical Properties

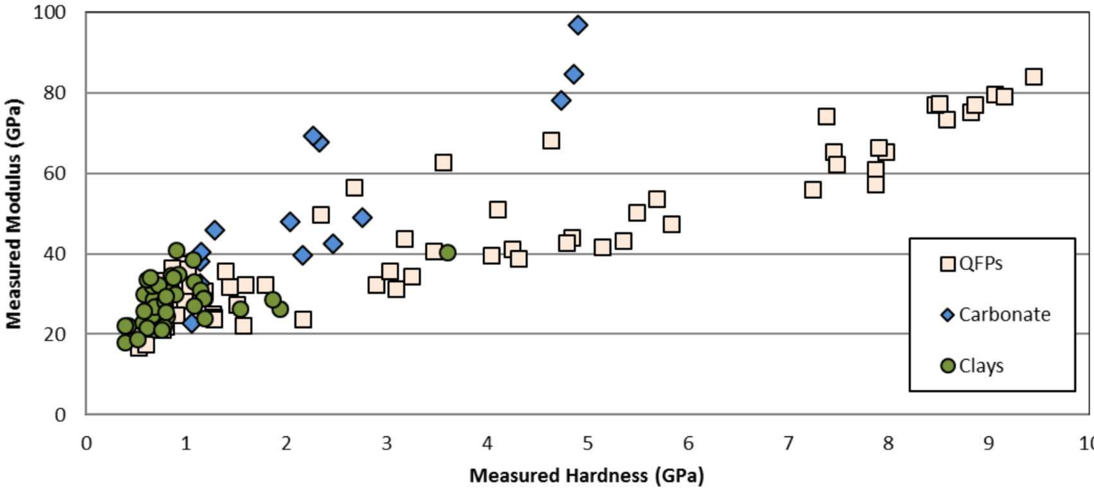

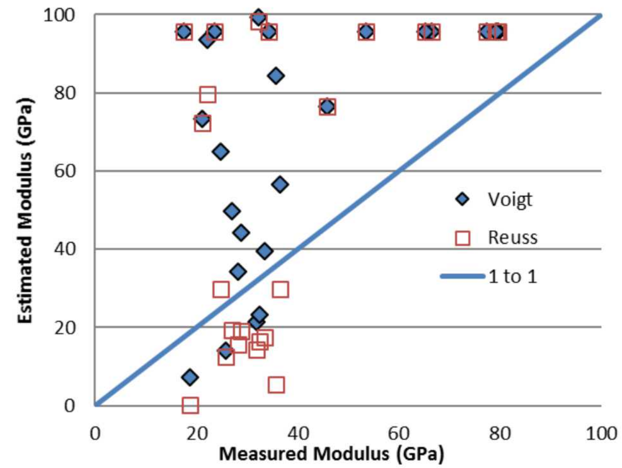

Sone & Zoback (2013)

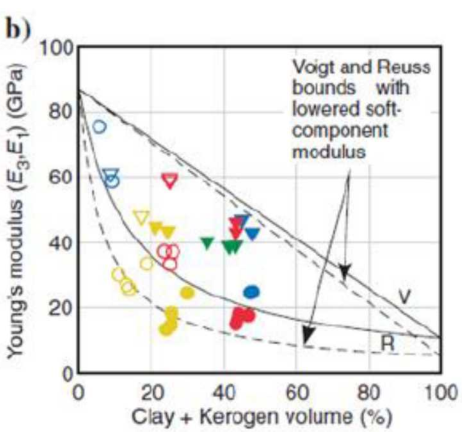

Shulka et al. (2013)

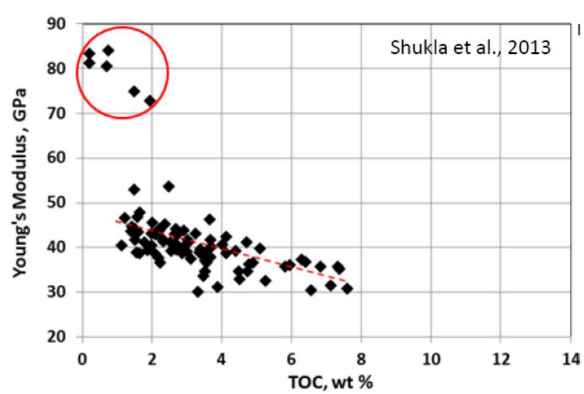

Kumar et al. (2012)

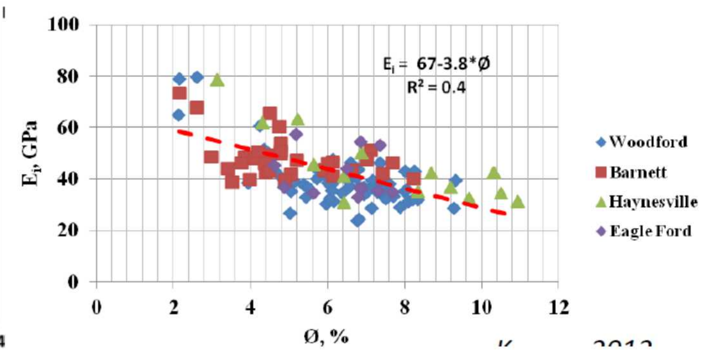

Nanoindentation Impressions

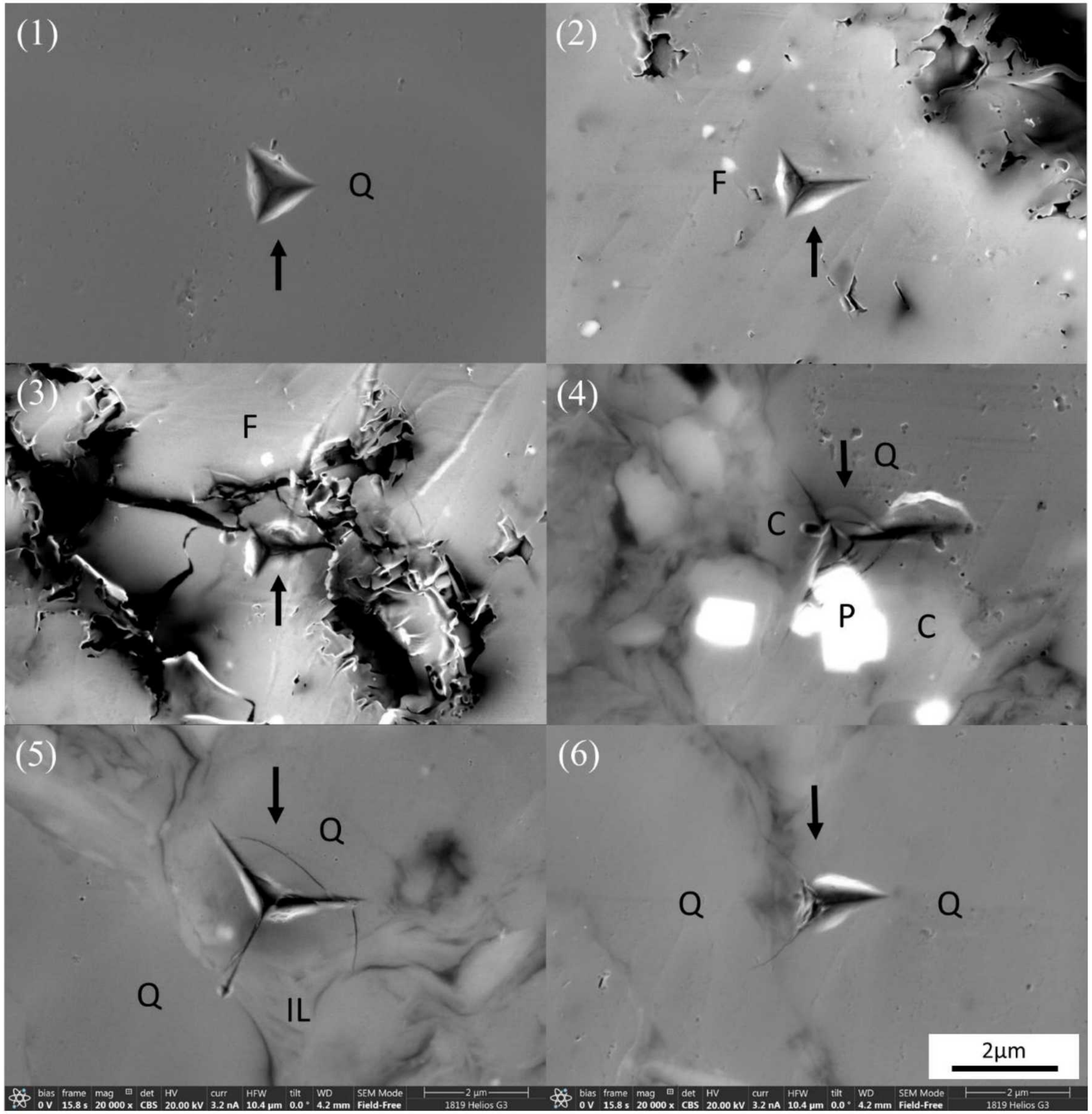

Low-clay percentage samples. (1&2): surface of pure quartz and feldspar having higher values of mechanical properties such as elastic modulus and hardness.
(3): dissolution surface of feldspar
(4-6): grain-to-grain boundary and edge-of-grain, which have lower mechanical properties values.

NOTE: Q=quartz, P=pyrite, C=carbonate, F=feldspar, and IL=illite)

Yoon et al. (in prep)

Effect of Compositions and textures on Mechanical Properties

High variability

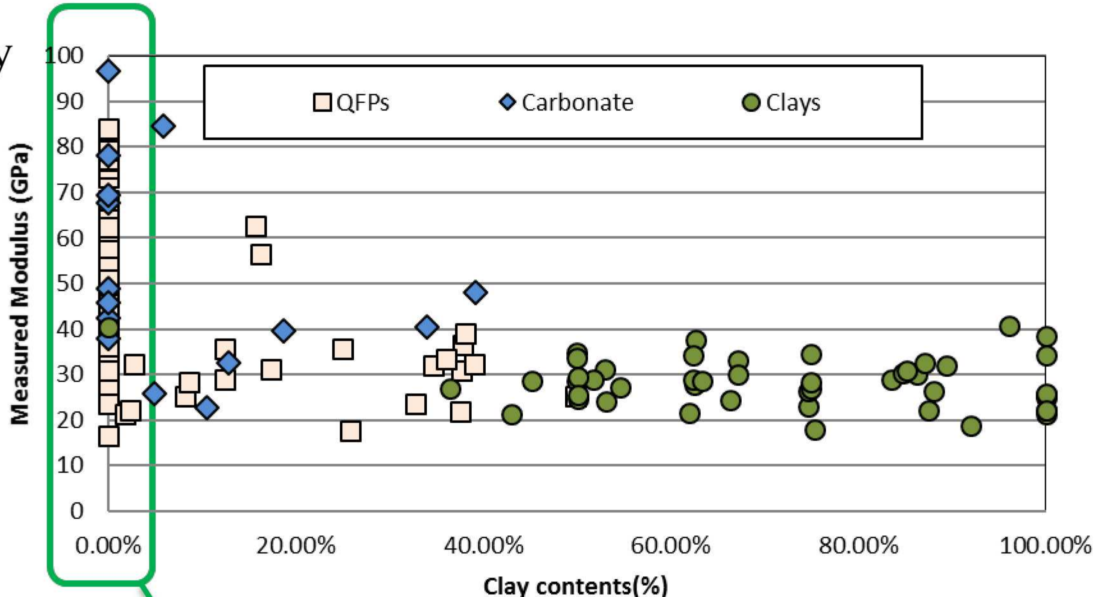

Analysis of SEM image on indentation impressions

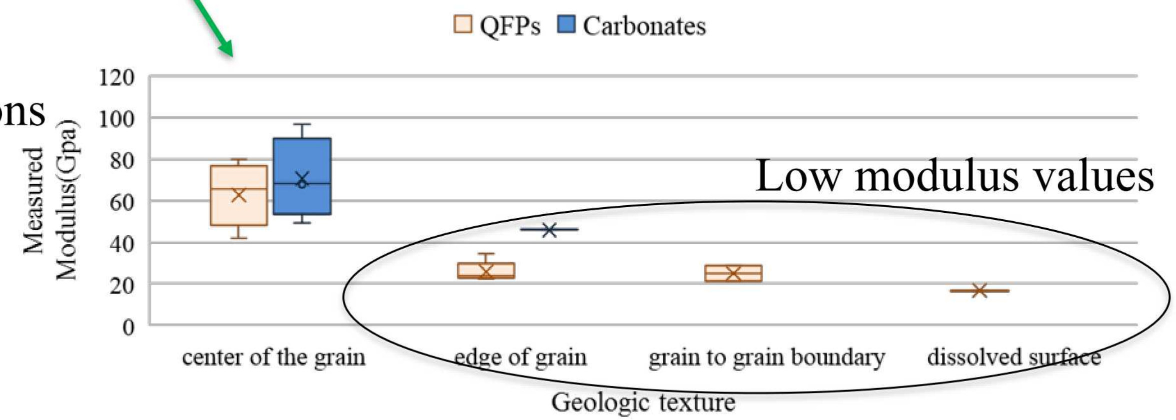

3D Mechanistic Modeling

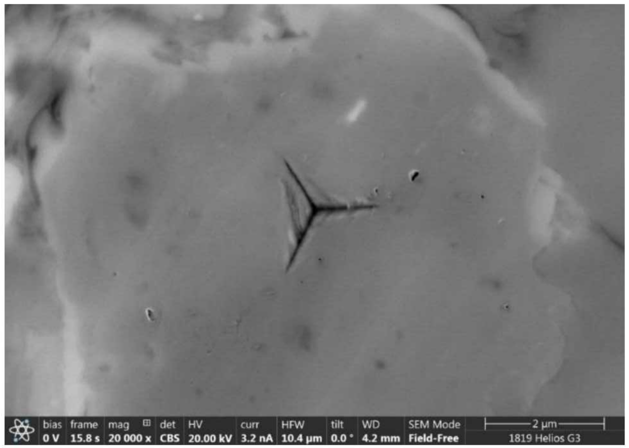

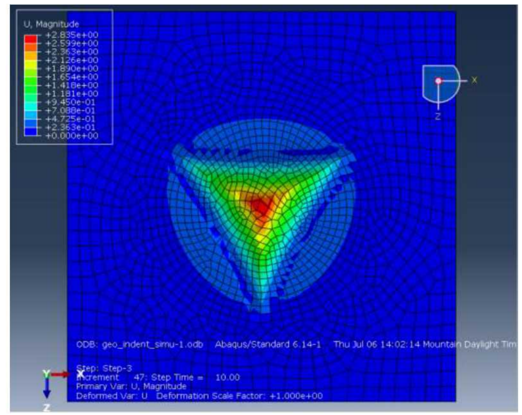

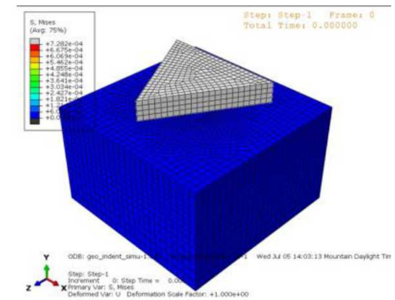

ABAQUS FEA

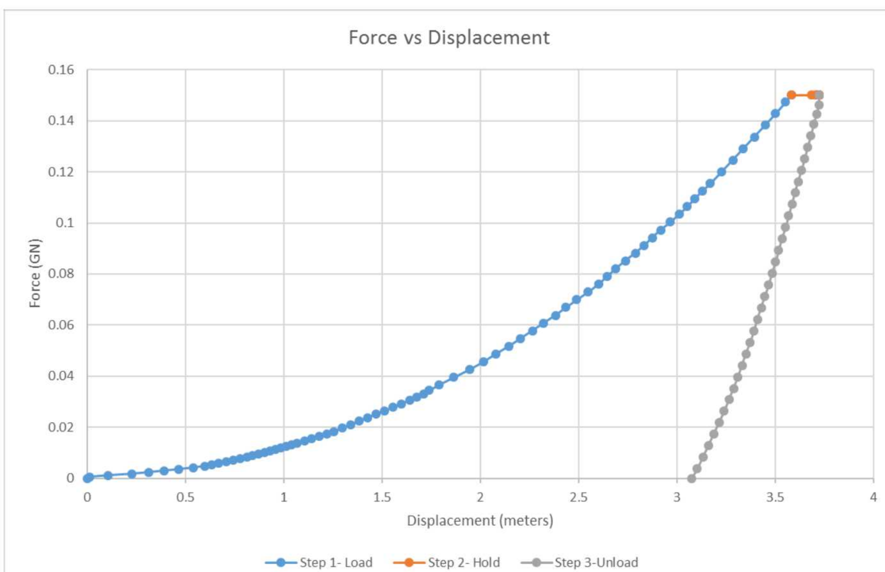

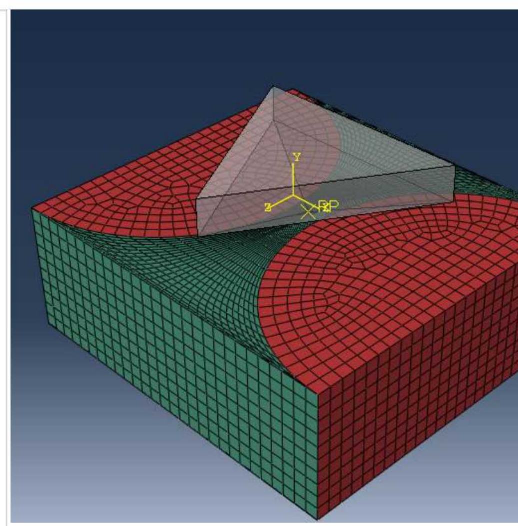

Elastic Modulus

Upscaling for Mechanical Properties

- Phase field modeling for averaging mechanical properties
  - Spatial mineralogical mapping with compositional heterogeneity
  - Development of correlation with nanoindentation results
  - Evaluation of soft cement or multi-mineral regions on mechanical responses with various conditions (e.g., defects, layering, anisotropy)

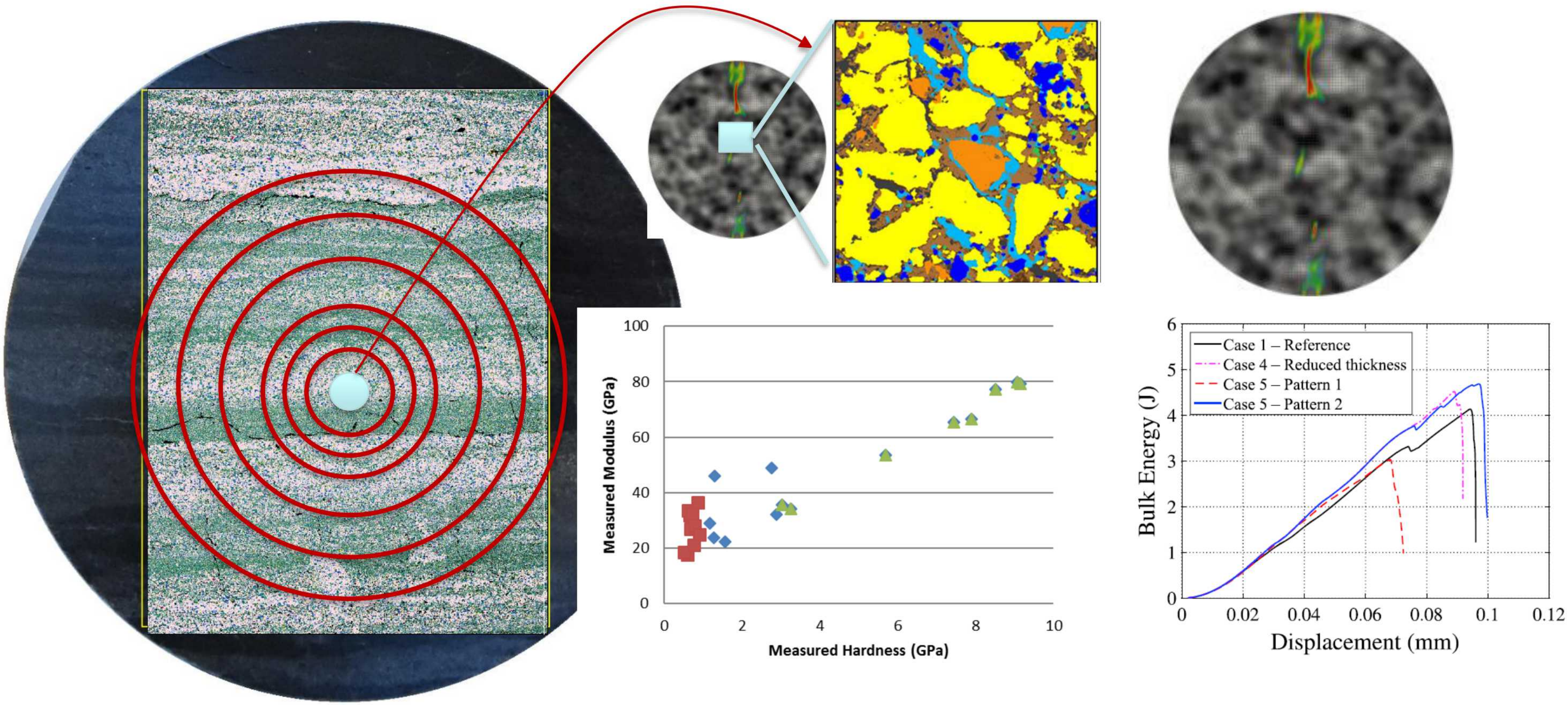

Velocities of Mancos Shale lithofacies

Drilled Core Samples

Lab Block Samples

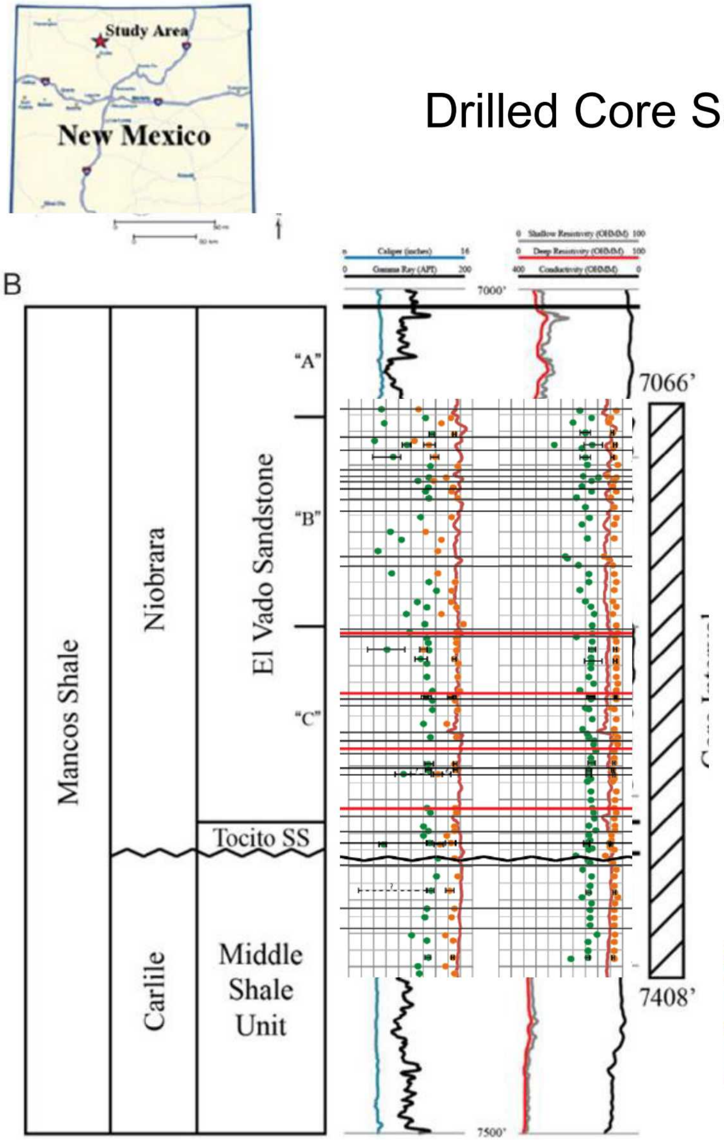

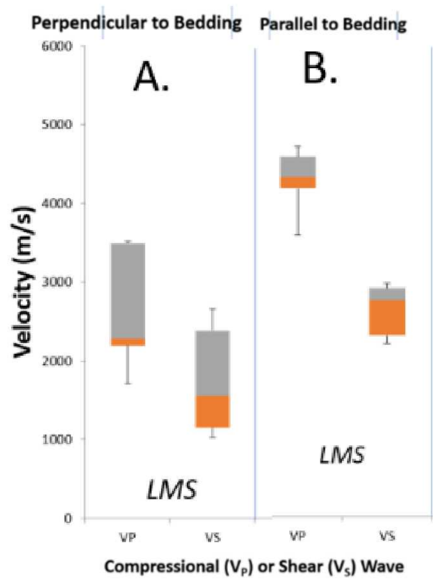

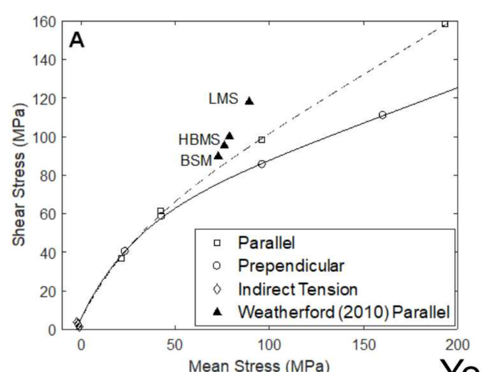

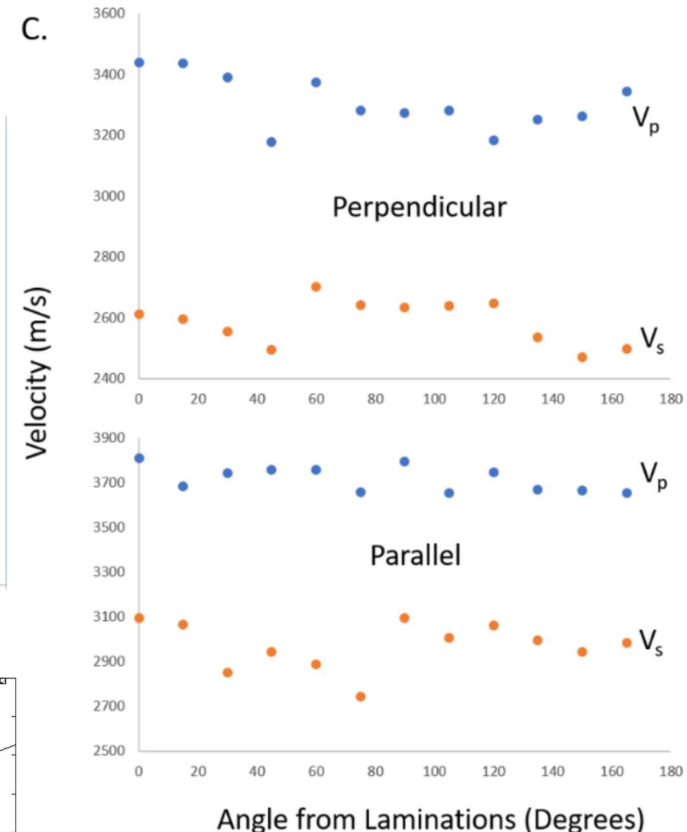

Yoon et al. (AAPG, Memoir 2019, in press)

Other Ongoing Works

Chemo-mechanical Processes: Chemical Flooding in Nano-porous Chalk

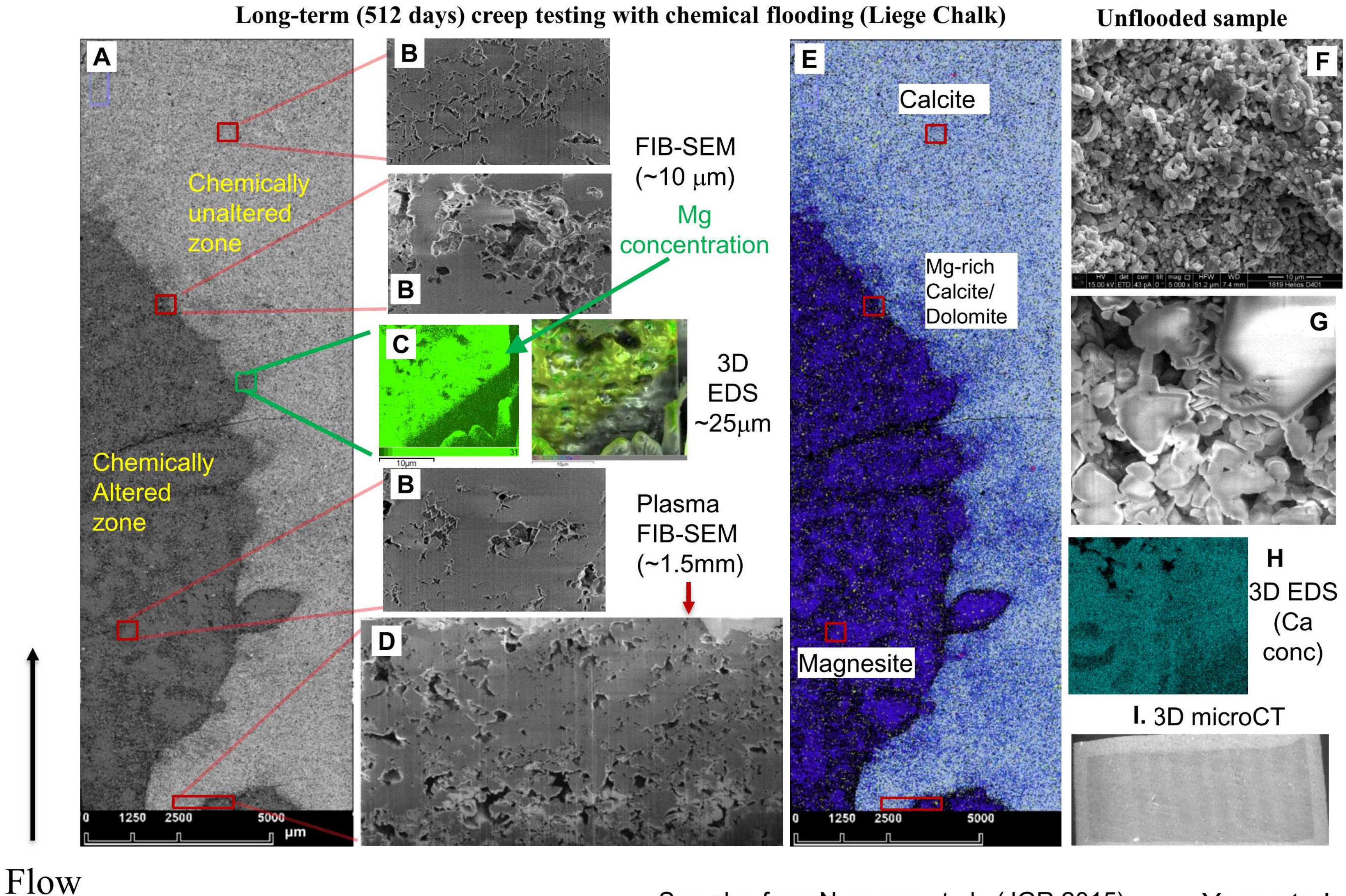

Samples from Nermoen et al., (JGR,2015)

Yoon et al. (In prep)

Fracture Patterns: Borehole Breakout Test

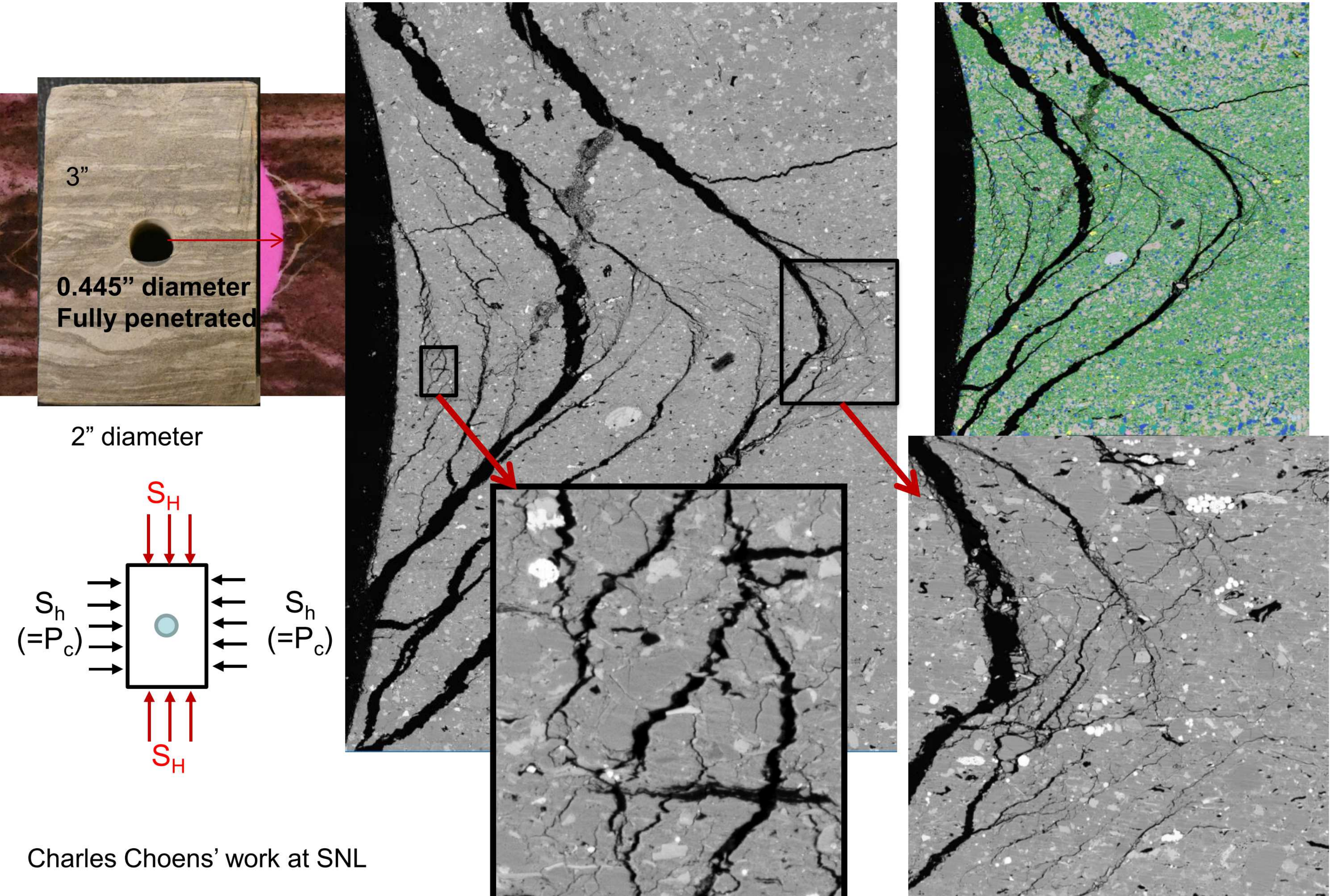

Charles Choens’ work at SNL

Permeability Control and Proppants' Behavior in Fractures

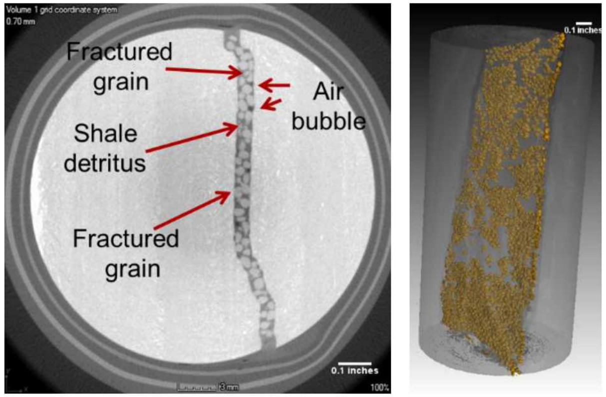

Micro-CT image with proppants in a fracture

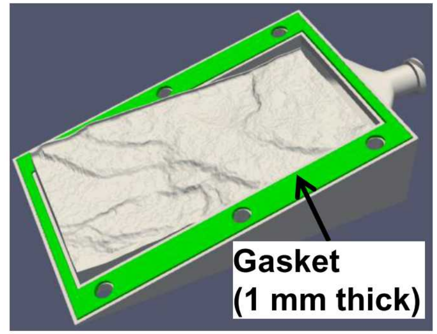

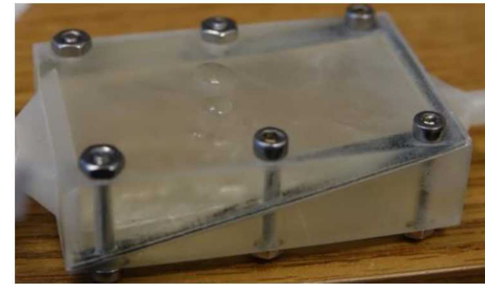

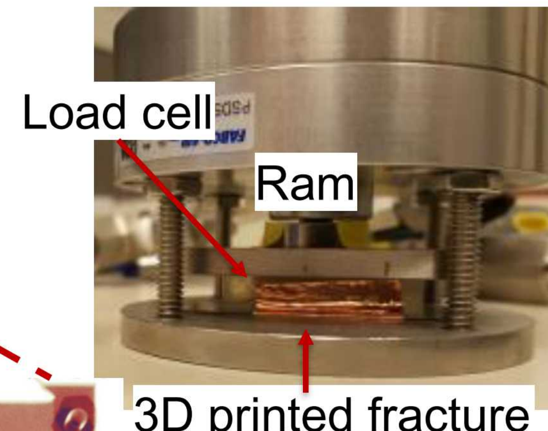

3D printing applications

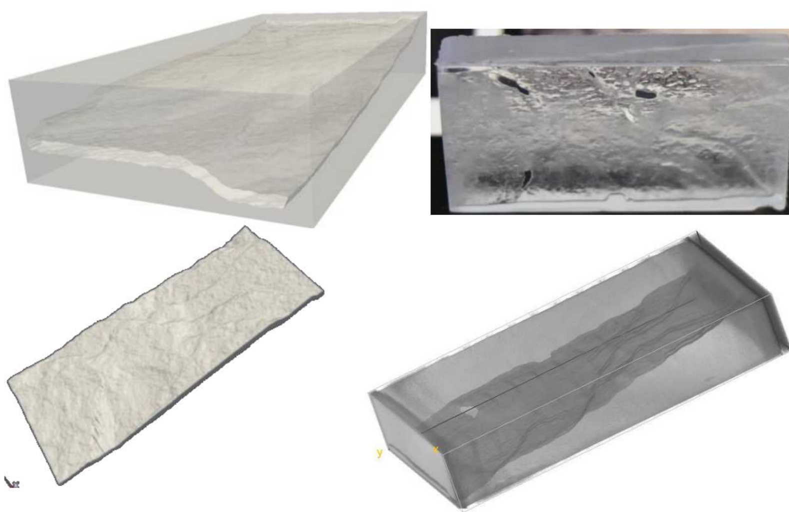

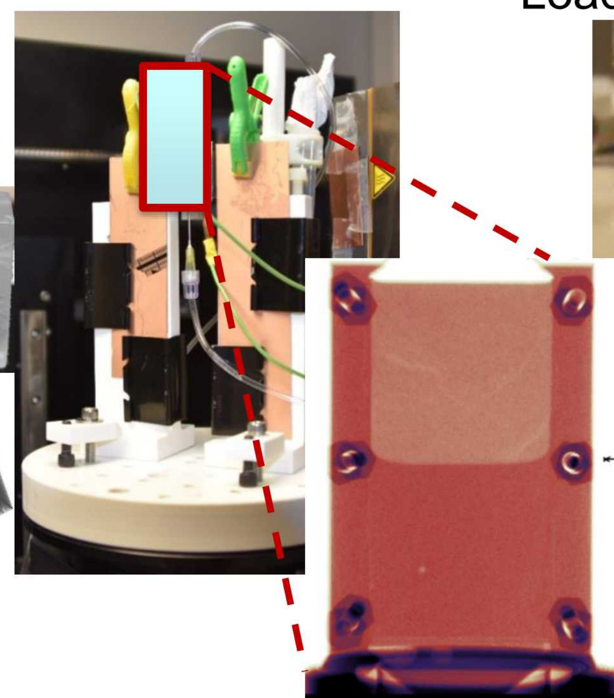

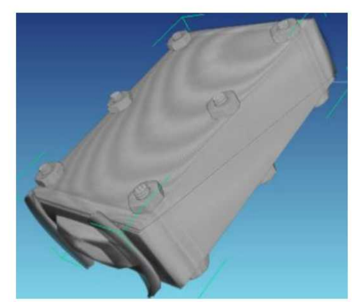

Multiphysics Simulations

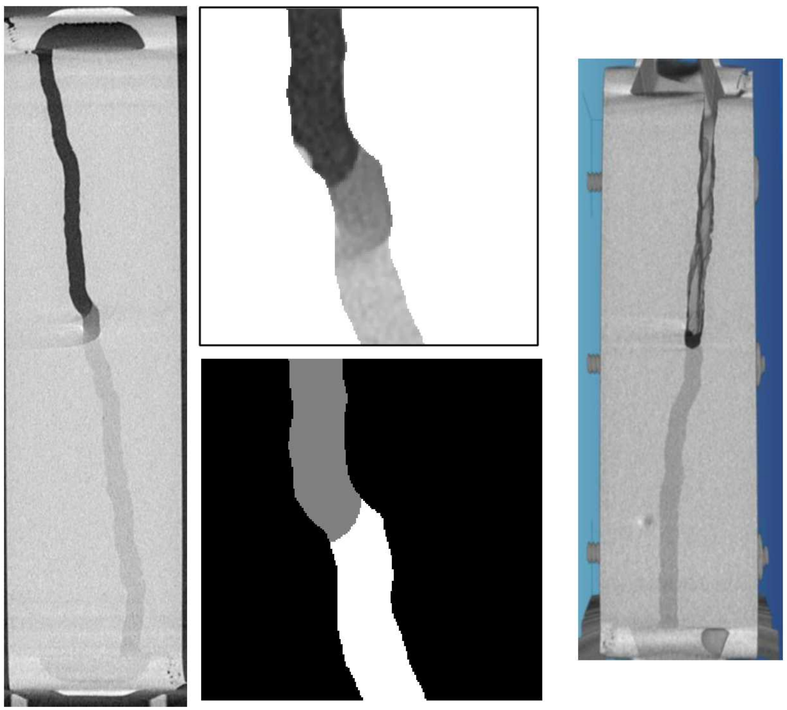

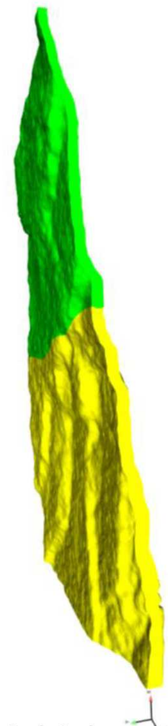

Multiphase flow

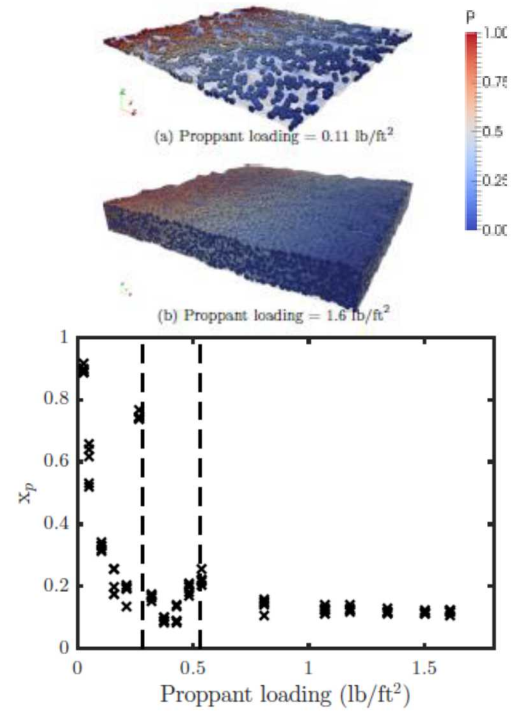

Proppants' behavior

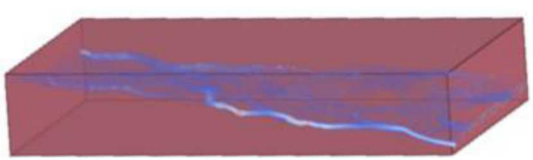

CFD simulation flow field

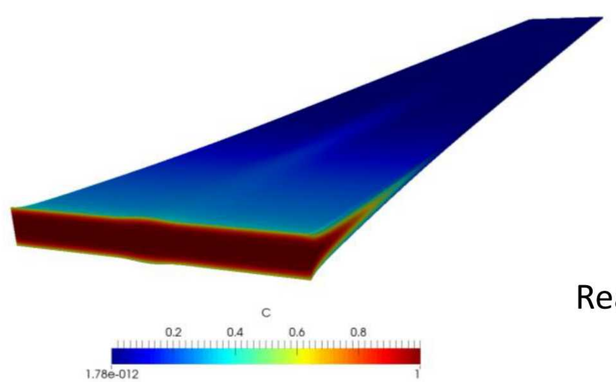

Reactive Transport

Methane flow in kerogen "tubule"

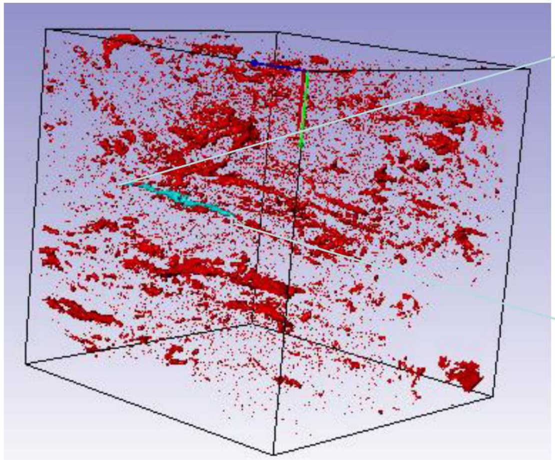

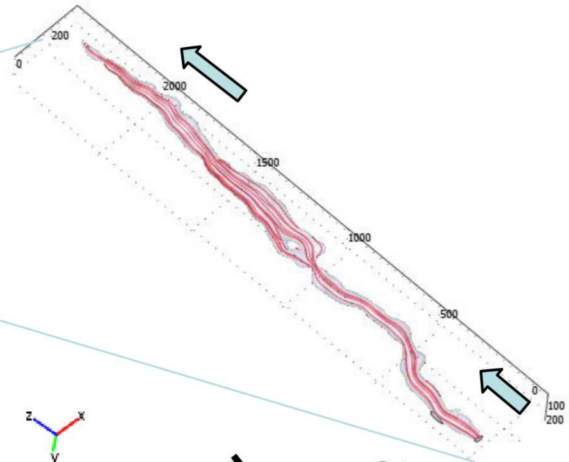

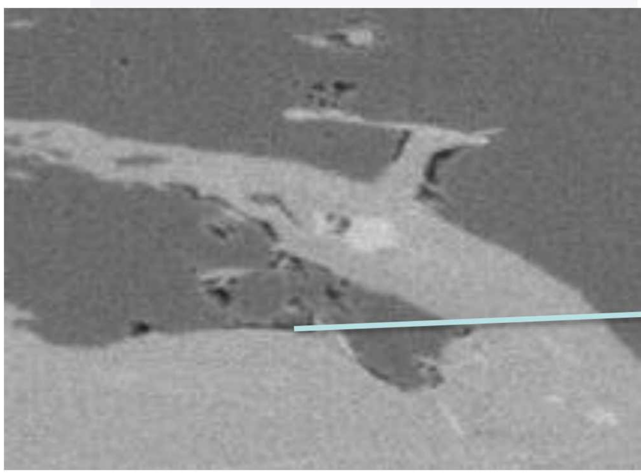

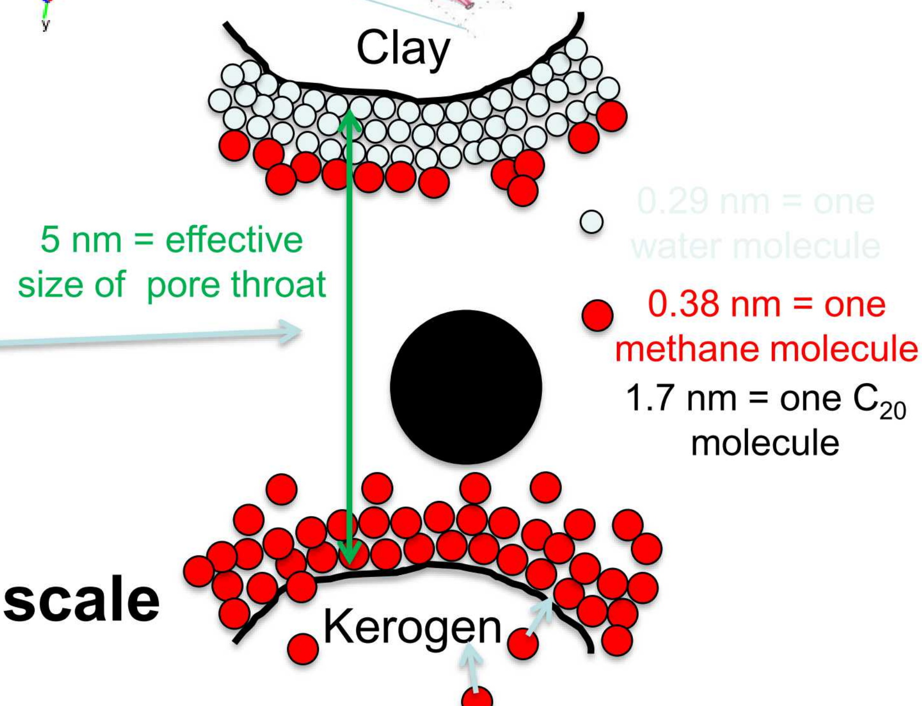

Pore throats are at molecular scale

Multiscale network and flows with ROMs + ML

Level 1:
- Nano/micro pore network (PN) & flow model
- Generative adversarial neural networks

Level 2:
- Natural/induced fracture network (FN) & flow model
- Graph network system

Level 3:
- Well production & operations
- Well systems + graph network under realistic operation conditions

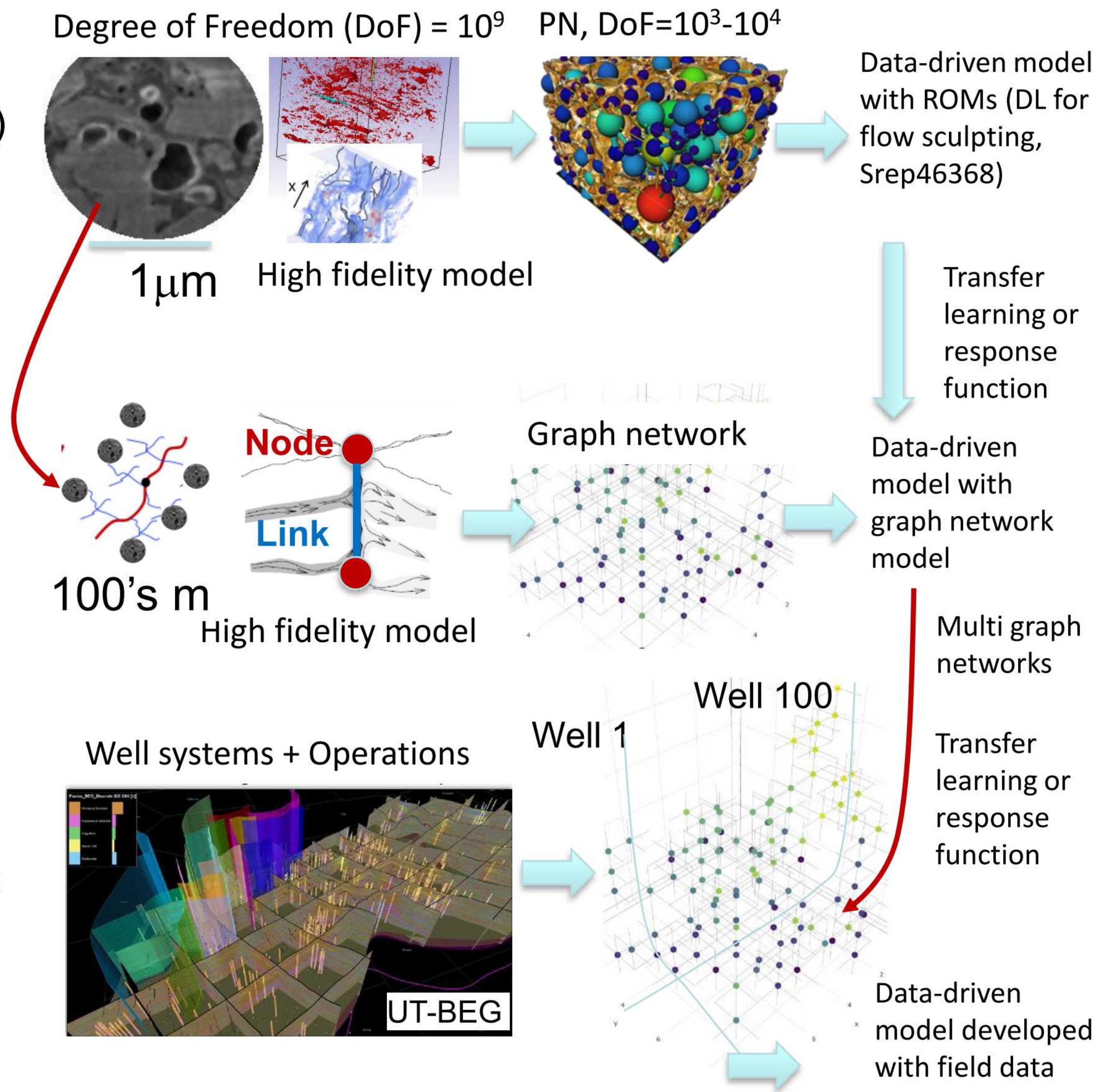

Refs: Yang et al. (2016) Srep36673; Wang et al. (2017); Brown (2006), Report DE-FG02-98ER14906

Summary

- Integrated multiscale imaging and mechanical testing with numerical simulation provides a robust approach to advancing our understanding of shale (poro-) mechanical behaviors
- Texture/mineralogical characterization
  – Recent advances in mineralogical mapping with high resolution imaging over the large area
  – Multiscale mineralogical and geologic features lead to considerable heterogeneity of mechanical properties
- Mechanical tests
  – Macroscopic and microscopic lithofacies have distinctively different mechanical properties
  – Bulk properties/averaging theory may be misleading as they can represent averages of mechanically heterogeneous rock
  – Microscopic heterogeneity of mechanical properties can control the spatial distribution of fractures
  – This heterogeneity should be taken into account for realistic mechanical modeling and can scale up by rigorous theoretical and numerical modeling